arXiv:0901.0012v1 [hep-th] 31 Dec 2008

Nucleon-Nucleon Potential from Holography

Keun-Young Kim and Ismail Zahed

Department of Physics and Astronomy, SUNY Stony-Brook, NY 11794

Abstract

In the holographic model of QCD, baryons are chiral solitons sourced by D4 flavor instantons in bulk of size $1/\sqrt{\lambda}$ with $\lambda = g^2 N_c$. Using the ADHM construction we explicit the exact two-instanton solution in bulk. We use it to construct the core NN potential to order N_c/λ. The core sources meson fields to order $\sqrt{N_c/\lambda}$ which are shown to contribute to the NN interaction to order N_c/λ. In holographic QCD, the NN interaction splits into a small core and a large cloud contribution in line with meson exchange models. The core part of the interaction is repulsive in the central, spin and tensor channels for instantons in the regular gauge. The cloud part of the interaction is dominated by omega exchange in the central channel, by pion exchange in the tensor channel and by axial-vector exchange in the spin and tensor channels. Vector meson exchanges are subdominant in all channels.

1 Introduction

Holographic QCD has provided an insightful look to a number of issues in baryonic physics at strong coupling $\lambda = g^2 N_c$ and large number of colors N_c [1, 2, 3, 4, 5, 6, 7, 8, 9, 10]. In particular, in [1, 2] baryons are constructed from a five-dimensional Shrodinger-like equation whereby the 5th dimension generates mass-like anomalous dimensions through pertinent boundary conditions. A number of baryonic properties have followed ranging from baryonic spectra to form factors [1, 2].

At large N_c baryons are chiral solitons in QCD. A particularly interesting framework for discussing this scenario is the D8-$\overline{\text{D8}}$ chiral holographic model recently suggested by Sakai and Sugimoto [11, 3] (herethrough hQCD). In hQCD D4 static instantons in bulk source the chiral solitons or Skyrmions on the boundary. The instantons have a size of order $1/\sqrt{\lambda}$ and a mass of order $N_c\lambda$ in units of M_{KK}, the Kaluza-Klein scale [3]. The static Skyrmion is just the instanton holonomy in the z-direction, with a larger size of order λ^0 [5].

In the past the Skyrmion-Skyrmion interaction was mostly analyzed using the product ansatz [12] or some variational techniques [13]. While the product ansatz reveals a pionic tail in the spin and tensor channels, it lacks the intermediate range attraction in the scalar channel expected from two-pion exchange. In fact the scalar potential to order N_c is found to be mostly repulsive, and therefore unsuited for binding nuclear matter at large N_c. The core part of the Skyrmion-Skyrmion interaction in the product of two Skyrmions is ansatz dependent. In [14] it was shown that the ansatz dependence could be eliminated in the two-pion range by adding the pion cloud to the core Skyrmions. In a double expansion using large N_c and the pion-range, a scalar attraction was shown to develop in the two-pion range in the scalar channel [14]. The expansion gets quickly involved while addressing shorter ranges or core interactions.

In this paper we analyze the two-baryon problem using the D4 two-instanton solution [15] to order N_c/λ. The ensuing Skyrmion-Skyrmion interaction is essentially that of the two cores and the meson cloud composed of (massles) pions and vector mesons. At strong coupling, holography fixes the core interactions in a way that the Skyrme model does not. Although in QCD very short ranged interactions are controlled by asymptotic freedom, the core interactions at intermediate distances maybe still in the realm of strong coupling and therefore unamenable to QCD perturbation theory. In this sense, holography will be helpful. Also, in holographic QCD the mesonic cloud including pions and vectors is naturally added to the core Skyrmions in the framework of semiclassics. These issues will be quantitatively addressed in this paper.

In section 2, we review the ADHM construction for one and two-instanton following on recent work in [15]. In section 3, we show how this construction translates to the one and two baryon configuration in holography. In section 4, we construct the bare or core Skyrmion-Skyrmion interaction for defensive and combed Skyrmions. We unwind the core Skyrmion-Skyrmion interaction at large separations in terms of a dominant Coulomb repulsion in regular gauge. Core issues related to the singular gauge are also discussed. In section 5, we project the core Skyrmion-Skyrmion contributions onto the core nucleon-nucleon contributions at large separation using semiclassics in the adiabatic approximation. In section 6, we include the effects of the mesonic cloud to order N_c/λ in the Born-Oppenheimer approximation. At large separations, the cloud contributions yield a tower of meson exchanges. In section 7, we summarize the general structure of the NN potential as a core plus cloud contribution in holographic QCD. Our conclusions are in section 8. In Appendix A we detail the $k = 1, 2$ instantons in the singular gauge. In Appendix B, we revisit the core interaction in the singular gauge. In Appendix C, we check our semiclassical cloud calculations in the regular gauge, using the strong coupling source theory in the singular gauge. In Appendix D we detail our nucleon axial-form factor and the extraction of the axial coupling g_A.

2 YM Instantons from ADHM

The starting point for baryons in holographic QCD are instantons in flat $R^3_X \times R_Z$. In this section we briefly review the ADHM construction [16] for SU(2) Yang-Mills instantons. Below SU(2) will be viewed as a flavor group associated to D8-$\overline{\text{D8}}$ branes. For a thorough presentation of the ADHM construction we refer to [17] and references therein.

In the ADHM construction, all the instanton information is encoded in the matrix-data whose elements are quaternions q. The latters are represented as

$$q \equiv q_M \sigma^M \ , \qquad \sigma^M \equiv (i\tau^i, \mathbb{1}) \ , \tag{1}$$

with $M = 1, 2, 3, 4$, $\mathbb{1} \equiv 1_{2\times 2}$, and τ^i the standard Pauli matrices. q_M are four real numbers. The conjugate ($q^\dagger$) and the modulus ($\|q\|$) of the quaternion, are defined as

$$q^\dagger \equiv q_M (\sigma^M)^\dagger \ , \quad \|q\|^2 \equiv q^\dagger q = q q^\dagger = |\,q|\,\mathbb{1} = \sum_M q_M^2 \mathbb{1} \ , \tag{2}$$

$$\mathrm{Re}\, q \equiv \frac{q + q^\dagger}{2} = q_0 \sigma^0 \ , \quad \mathrm{Im}\, q \equiv \frac{q - q^\dagger}{2} = \sum_i q_i \sigma^i \ , \tag{3}$$

where $|\,q|$ is the determinant of a matrix q. For clarity, our label conventions are: $M, N, P, Q \in \{1,2,3,4\}$, $\mu,\nu,\rho,\sigma, \in \{0,1,2,3\}$, and $i,j,k,l \in \{1,2,3\}$ with $z \equiv x_4$. The flavor $SU(2)$ group indices are $a, b \in \{1,2,3\}$.

The basic block in the matrix-data is the $(1+k)\times k$ matrix, Δ, for the charge k instanton

$$\Delta = \mathbb{A} + \mathbb{B} \otimes x \ , \tag{4}$$

where $\mathbb{A}$ and $\mathbb{B}$ are x-independent $(1+k)\times k$ quaternionic matrices with information on the moduli parameters. We define $x = x_M \sigma^M$ and $\mathbb{B}\otimes x$ means that each element $\mathbb{B}$ is multiplied by x. $\mathbb{A}$ and $\mathbb{B}$ are not arbitrary. They follow from the ADHM constraint

$$\Delta^\dagger \Delta = f^{-1} \otimes \mathbb{1} \ , \tag{5}$$

where $\Delta^\dagger$ is the transpose of the quaternionic conjugate of Δ. f is a $k\times k$ invertible quaternionic matrix. $f^{-1}\otimes\mathbb{1}$ means each element f^{-1} is multiplied by $\mathbb{1}$. The null-space of $\Delta^\dagger$ is 2-dimensional since it has 2 fewer rows than columns. The basis vectors for this null-space can be assembled into an $(1+k)\times 1$ quaternionic matrix U

$$\Delta^\dagger U = 0 \ , \tag{6}$$

where U is normalized as

$$U^\dagger U = \mathbb{1} \ . \tag{7}$$

The instanton gauge field A_μ is constructed as

$$A_M = i U^\dagger \partial_M U \ , \tag{8}$$

which yields the field strengths

$$F_{MN} = -2\eta_{aMN} U^\dagger \mathbb{B}(f\otimes\tau^a)\mathbb{B}^\dagger U \ . \tag{9}$$

Self-duality is explicit from 't Hooft's self-dual eta symbol

$$\eta_{aMN} = -\eta_{aNM} = \begin{cases} \epsilon_{aMN} & \text{for } M,N = 1,2,3 \\ \delta_{aM} & \text{for } N = 4 \end{cases} \ . \tag{10}$$

The action density, $\mathrm{tr}\, F_{MN}^2$, can be calculated directly from f, without recourse to the null-space U and F_{MN} [18]

$$\mathrm{tr}\, F_{MN}^2 = \Box^2 \log |f| \ , \tag{11}$$

where $\Box \equiv \partial_M^2$, $\Box^2 = \partial_N^2 \partial_M^2$, and $|f|$ is the determinant of f.

2.1 $k = 1$ instanton

The $k = 1$ instanton in the regular gauge is encoded in a quaternionic matrix Δ

$$\Delta \equiv \begin{pmatrix} \lambda \\ -x + X \end{pmatrix} \ , \qquad \Delta^\dagger \equiv \begin{pmatrix} \lambda^\dagger & (-x + X)^\dagger \end{pmatrix} \ , \tag{12}$$

which yields

$$f^{-1} = \rho^2 + (x_M - X_M)^2 \ , \tag{13}$$

after using (5). Here ρ ($=\sqrt{\lambda_M^2}$) is the size and $\{X_M\}$ is the position of the one instanton. The field strength is

$$F_{MN} = W \eta_{aMN} \frac{\tau^a}{2} \frac{-4\rho^2}{((x_M - X_M)^2 + \rho^2)^2} W^\dagger \ , \tag{14}$$

which follows from (9) with

$$U = \frac{\rho}{\sqrt{(x_M - X_M)^2 + \rho^2}} \begin{pmatrix} -\frac{\lambda (x - X)^\dagger}{\rho^2} \\ \mathbb{1} \end{pmatrix} W^\dagger \ , \qquad B = \begin{pmatrix} 0 \\ -\mathbb{1} \end{pmatrix} \ , \tag{15}$$

where $\rho^2 \equiv \lambda^\dagger \lambda$ and $W \in SU(2)$. The action density follows from (14) or (11)

$$\mathrm{tr}\, F_{MN}^2 = \Box^2 \log f \ = \frac{96 \rho^4}{((x_M - X_M)^2 + \rho^2)^4}, \tag{16}$$

which gives the instanton number $\frac{1}{16\pi^2} \int d^4x \mathrm{tr}\, F_{MN}^2 = 1$ by self duality. The $k = 1$ instanton in the singular gauge is detailed in Appendix A.

2.2 $k = 2$ instanton

A charge 2 ($k = 2$) instanton in the regular gauge is encoded in a quaternionic matrix Δ [15]

$$\Delta \equiv \begin{pmatrix} \lambda_1 & \lambda_2 \\ -\big[x-(X+D)\big] & u \\ u & -\big[x-(X-D)\big] \end{pmatrix} \ , \tag{17}$$

where the coordinates x_M are defined as $x = x_M \sigma^M$, and the moduli parameters are encoded in the free parameters $\lambda_1, \lambda_2, X, D$: $|\lambda_i| \equiv \rho_i \mathbb{1}$ are the size parameters, $\lambda_1^\dagger \lambda_2/(\rho_1\rho_2) \in SU(2)$ is the relative gauge orientation, and $X \pm D$ is the location of the constituents. u is not a free parameter and will be determined in terms of other moduli parameters by the ADHM constraint (5).

Since we are interested in the relative separation we set $X = 0$, so that

$$\Delta = \begin{pmatrix} \lambda_1 & \lambda_2 \\ D-x & u \\ u & -D-x \end{pmatrix} \ , \qquad \Delta^\dagger \equiv \begin{pmatrix} \lambda_1^\dagger & (D-x)^\dagger & u^\dagger \\ \lambda_2^\dagger & u^\dagger & (-D-x)^\dagger \end{pmatrix} \ , \tag{18}$$

which yields

$$\Delta^\dagger \Delta = \begin{pmatrix} \|\lambda_1\|^2 + \|x-D\|^2 + \|u\|^2 & \lambda_1^\dagger \lambda_2 + D^\dagger u - u^\dagger D - (x^\dagger u + u^\dagger x) \\ \big[\lambda_1^\dagger \lambda_2 + D^\dagger u - u^\dagger D - (x^\dagger u + u^\dagger x)\big]^\dagger & \|\lambda_2\|^2 + \|x+D\|^2 + \|u\|^2 \end{pmatrix} \ . \tag{19}$$

The ADHM constraint (5) implies that each entry must be proportional to $\mathbb{1}$. The diagonal terms satisfy the constraint. The off-diagonal entries are also proportional to $\mathbb{1}$ provided that u is chosen to be

$$u = \frac{D\Lambda}{2\,|D|^2} + \gamma D \ , \qquad \Lambda \equiv \mathrm{Im}(\lambda_2^\dagger \lambda_1) = \frac{1}{2}(\lambda_2^\dagger \lambda_1 - \lambda_1^\dagger \lambda_2) \ , \tag{20}$$

with γ an arbitrary real constant. The coordinate u is the inverse of the coordinate D. It plays the role of the dual distance. Throughout we follow [15] and choose $\gamma = 0$ for a *physical identification of the moduli parameters.* By that we mean a $k = 2$ configuration which is the closest to the superposition of two instantons in the regular gauge at large separation. In Appendix A, we briefly discuss a minimal $k = 2$ configuration in the singular gauge.

Inserting u into (19) yields

$$f^{-1} = \begin{pmatrix} \rho_1^2 + (x_M - D_M)^2 + \frac{\rho_1^2\rho_2^2 - (\lambda_1\cdot\lambda_2)^2}{4D_M^2} & \lambda_1\cdot\lambda_2 + 2x\cdot u \\ \lambda_1\cdot\lambda_2 + 2x\cdot u & \rho_2^2 + (x_M + D_M)^2 + \frac{\rho_1^2\rho_2^2 - (\lambda_1\cdot\lambda_2)^2}{4D_M^2} \end{pmatrix} , \qquad (21)$$

where we introduced the notation $q \cdot p$ for two quaternions q and p

$$q \cdot p \equiv \sum_M q_M p_M \ . \qquad (22)$$

$\rho_i = \sqrt{\lambda_i \cdot \lambda_i}$ are the size parameters, $\pm D_M$ the relative positions of the instantons, and

$$2x \cdot u = \frac{1}{D\cdot D}\left[(\lambda_2\cdot D)(\lambda_1\cdot x) - (\lambda_1\cdot D)(\lambda_2\cdot x) - \epsilon^{MNPQ}(\lambda_2)_M(\lambda_1)_N D_P x_Q\right] \ . \qquad (23)$$

We made use of the identity

$$\begin{aligned} \sigma^P\bar{\sigma}^{MN} &= \delta^{PM}\sigma^N - \delta^{PN}\sigma^M - \epsilon^{PMNQ}\sigma^Q \ , \\ \bar{\sigma}^{MN} &\equiv \frac{1}{2}(\bar{\sigma}^M\sigma^N - \bar{\sigma}^N\sigma^M) \ , \quad \epsilon^{1234} = 1 \ . \end{aligned} \qquad (24)$$

2.3 Explicit Parametrization

Without loss of generality, we may choose the moduli parameters to be

$$\lambda_1 = \rho_1\,(0,0,0,1) \ , \quad \lambda_2 = \rho_2\left(\widehat{\theta}_a \sin|\,\theta|\,, \cos|\,\theta|\right) \ , \quad D = \left(\frac{d}{2}, 0, 0, 0\right) \ , \qquad (25)$$

with $a = 1,2,3$, $|\,\theta| \equiv \sqrt{(\theta_1)^2 + (\theta_2)^2 + (\theta_3)^2}$ and $\widehat{\theta}_a \equiv \frac{\theta_a}{|\theta|}$. The spatial x^1 axis is chosen as the separation axis of two instantons at large distance d. The flavor orientation angles (θ_a) are relative to the λ_1 orientation. We assign an $SU(2)$ matrix U to the relative angle orientations in flavor space

$$U \equiv \frac{\lambda_1^\dagger \lambda_2}{\rho_1\rho_2} = e^{i\theta_a\tau^a} \in SU(2) \ , \qquad (26)$$

which is associated with the orthogonal $SO(3)$ rotation matrix R as

$$\begin{aligned} R_{ab} &= \frac{1}{2}\text{tr}\,\left(\tau_a U \tau_b U^\dagger\right) \\ &= \delta_{ab}\cos 2|\,\theta| + 2\widehat{\theta}_a\widehat{\theta}_b\sin^2|\,\theta| + \epsilon_{abc}\widehat{\theta}_c \sin 2|\,\theta| \ . \end{aligned} \qquad (27)$$

For instance R_{ab} reads

$$\begin{pmatrix} \cos 2\theta_3 & \sin 2\theta_3 & 0 \\ -\sin 2\theta_3 & \cos 2\theta_3 & 0 \\ 0 & 0 & 1 \end{pmatrix} \ , \qquad \begin{pmatrix} 1 & 0 & 0 \\ 0 & \cos 2\theta_1 & \sin 2\theta_1 \\ 0 & -\sin 2\theta_1 & \cos 2\theta_1 \end{pmatrix} \ , \tag{28}$$

for $\theta_1 = \theta_2 = 0$ and $\theta_2 = \theta_3 = 0$ respectively. Note the double covering in going from SU(2) to SO(3).

In this coordination for the moduli space,

$$\Lambda = \rho_1 \mathrm{Im}(\lambda_2^\dagger) = \rho_1\rho_2(-i\widehat{\theta}_a \tau^a \sin|\,\theta|) \ , \tag{29}$$

$$u = \frac{D\Lambda}{2\,|D|^2} = \frac{i\tau^1\Lambda}{d} = \frac{\rho_1\rho_2}{d} \sin|\,\theta|\,\widehat{\theta}_a \tau^1 \tau^a \ , \tag{30}$$

$$u_M = \frac{\rho_1\rho_2}{d} \sin|\,\theta| \left(0, -\widehat{\theta}_3, \widehat{\theta}_2, \widehat{\theta}_1\right) \ , \tag{31}$$

$$x \cdot u = \frac{\rho_1\rho_2 \sin|\,\theta|}{d} \left(\widehat{\theta}_1 x_4 + \widehat{\theta}_2 x_3 - \widehat{\theta}_3 x_2\right) \ , \tag{32}$$

and the inverse potential f^{-1} is written as

$$f^{-1} = \begin{pmatrix} g_- + A & B \\ B & g_+ + A \end{pmatrix} \ , \tag{33}$$

$$g_\pm \equiv x_\alpha^2 + \left(x_1 \pm \frac{d}{2}\right)^2 + \rho^2 \ , \quad x_\alpha^2 \equiv x_2^2 + x_3^2 + x_4^2 \ , \tag{34}$$

$$A \equiv \frac{\rho^4 \sin^2|\,\theta|}{d^2} \ , \quad B \equiv \rho^2 \left(\cos|\,\theta| + \frac{2}{d} \sin|\,\theta| \left[\widehat{\theta}_1 z + \widehat{\theta}_2 x_3 - \widehat{\theta}_3 x_2\right]\right) \ , \tag{35}$$

with $\rho \equiv \rho_1 = \rho_2$. The action density can be assessed using (11). In terms of this notation, for the $k = 1$ instanton in the regular gauge (13), the logarithmic potential $\log|f|$ is

$$\log f_\pm = -\log g_\pm \ , \tag{36}$$

where the subscript ± refers to the position $\mp\frac{d}{2}$ of the instanton along the x_1 axis. For the $k = 2$ instanton (33), we have

$$\log|f_{-+}| \ \equiv \ -\log\left[(g_- + A)(g_+ + A) - B^2\right] \ . \tag{37}$$

2.4 Asymptotics

To understand in details the structure of the $k = 2$ instanton it is best to work out its asymptotic form for the case $d/\rho \gg 1$. For that we use (9) in the special case

$$F_{iz} = -2U^\dagger \mathbb{B}(f \otimes \tau^i)\mathbb{B}^\dagger U \ , \tag{38}$$

with

$$\mathbb{B} = \begin{pmatrix} 0 & 0 \\ -\mathbb{1} & 0 \\ 0 & -\mathbb{1} \end{pmatrix} . \tag{39}$$

Below, we will show that the field strength F_{iz} sources the pion-nucleon coupling in the axial gauge $A_z = 0$ for the quantum fluctuations. The asymptotics is useful for a physical identification of the coset parameters.

Near the singularity center with $x = D$, (18) approximates to

$$\Delta^\dagger \approx \begin{pmatrix} \lambda_1^\dagger & 0 & u^\dagger \\ \lambda_2^\dagger & u^\dagger & -2D^\dagger \end{pmatrix} , \tag{40}$$

whose null vector U is

$$U \approx \begin{pmatrix} -\frac{1}{\rho_1} u^\dagger \\ \frac{1}{|u|^2}\frac{1}{\rho_1} u \left(\lambda_2^\dagger u^\dagger + 2\rho_1 D^\dagger\right) \\ \mathbb{1} \end{pmatrix} D\Lambda^\dagger D^\dagger. \tag{41}$$

From (7) and (20) it follows that

$$U \approx \begin{pmatrix} 0 \\ \mathbb{1} - \left(\frac{\rho}{d}\right)^2 \frac{1}{2} \sin 2|\theta|\, \widehat{\theta}_a (i\tau^1\tau^a\tau^1) \\ \left(\frac{\rho}{d}\right)^2 \sin|\theta|\, \widehat{\theta}_a (i\tau^1\tau^a\tau^1) \end{pmatrix} + \begin{pmatrix} \mathcal{O}\left(\frac{\rho}{d}\right)^3 \\ \mathcal{O}\left(\frac{\rho}{d}\right)^4 \\ \mathcal{O}\left(\frac{\rho}{d}\right)^4 \end{pmatrix} . \tag{42}$$

We have used the explicit parametrization (25) and (29). We may expand f near the center $X = D$,

$$f|_{X\approx D} = \begin{pmatrix} \frac{1}{g_+} + \mathcal{O}\left(\frac{1}{d}\right)^4 & -\frac{\lambda_1\lambda_2 + 2x\cdot u}{g_- g_+} + \mathcal{O}\left(\frac{1}{d}\right)^4 \\ -\frac{\lambda_1\lambda_2 + 2x\cdot u}{g_- g_+} + \mathcal{O}\left(\frac{1}{d}\right)^4 & \frac{1}{g_-} + \mathcal{O}\left(\frac{1}{d}\right)^2 \end{pmatrix} . \tag{43}$$

For $X = D$, the leading contributions to f_{11}, f_{12}, and f_{21} are of order $1/d^2$ while that of f_{22} is of order d^0.

From (39) and (42) we have

$$U^\dagger B|_{X\approx D} = \left(-\mathbb{1} + \mathcal{O}\left(\frac{\rho}{d}\right)^2, \mathcal{O}\left(\frac{\rho}{d}\right)^2\right) \equiv \left(\mathfrak{b}_1^\dagger, \mathfrak{b}_2^\dagger\right) \;, \tag{44}$$

which yields (38)

$$\begin{aligned} F_{iz}|_{X\approx D} &= -2U^\dagger B(f\otimes\tau^i)B^\dagger U|_{X\approx D} \\ &= -2\left(f_{11}\mathfrak{b}_1^\dagger\tau^i\mathfrak{b}_1 + f_{12}\mathfrak{b}_1^\dagger\tau^i\mathfrak{b}_2 + f_{21}\mathfrak{b}_2^\dagger\tau^i\mathfrak{b}_1 + f_{22}\mathfrak{b}_2^\dagger\tau^i\mathfrak{b}_2\right) \\ &= -2\frac{\tau^i}{g_+} + \mathcal{O}(d^{-4}) \;. \end{aligned} \tag{45}$$

Thus

$$F^a_{iz}|_{X\approx D} \approx -2\delta^{ia}\frac{1}{g_+} \tag{46}$$

A rerun of the argument for the center $x = -D$ yields

$$F^a_{iz}|_{X\approx -D} \approx -2R^{ia}\frac{\tau^i}{g_-} \;, \tag{47}$$

since $U^\dagger \sim (0, 0, \mathbb{1})$. For asymptotic distances $d/\rho \gg 1$ the $k = 2$ configuration splits into two independent $k = 1$ configurations with relative flavor orientation R^{ab}. This separation makes explicit the physical interpretation of the coset parameters: ρ the instanton size, d the instanton relative separation, u the inverse or dual separation and R their relative orientations asymptotically.

3 Baryons in hQCD

Baryons in hQCD are sourced by instantons in bulk. The induced action by pertinent brane embeddings and its instanton content was discussed in [3]. The 5D *effective* Yang-Mills action is the leading terms in the $1/\lambda$ expansion of the DBI action of the D8 branes after integrating out the S^4. The 5D Chern-Simons action is obtained from the Chern-Simons action of the D8 branes by integrating F_4 RR flux over the S^4, which is nothing but N_C.

The action reads [11, 3]

$$S = S_{YM} + S_{CS} \ , \tag{48}$$
$$S_{YM} = -\kappa \int d^4x dz \ \mathrm{tr} \left[\frac{1}{2} K^{-1/3} \mathcal{F}_{\mu\nu}^2 + M_{\mathrm{KK}}^2 K \mathcal{F}_{\mu z}^2 \right] \ , \tag{49}$$
$$S_{CS} = \frac{N_c}{24\pi^2} \int_{M^4 \times R} \omega_5^{U(N_f)}(\mathcal{A}) \ , \tag{50}$$

where $\mu, \nu = 0, 1, 2, 3$ are 4D indices and the fifth(internal) coordinate z is dimensionless. There are three things which are inherited by the holographic dual gravity theory: M_{KK}, κ, and K. M_{KK} is the Kaluza-Klein scale and we will set $M_{\mathrm{KK}} = 1$ as our unit. κ and K are defined as

$$\kappa = \lambda N_c \frac{1}{216\pi^3} \equiv \lambda N_c a \ , \qquad K = 1 + z^2 \ . \tag{51}$$

$\mathcal{A}$ is the 5D $U(N_f)$ 1-form gauge field and $\mathcal{F}_{\mu\nu}$ and $\mathcal{F}_{\mu z}$ are the components of the 2-form field strength $\mathcal{F} = \mathrm{d}\mathcal{A} - i\mathcal{A} \wedge \mathcal{A}$. $\omega_5^{U(N_f)}(\mathcal{A})$ is the Chern-Simons 5-form for the $U(N_f)$ gauge field

$$\omega_5^{U(N_f)}(\mathcal{A}) = \mathrm{tr} \left(\mathcal{A}\mathcal{F}^2 + \frac{i}{2}\mathcal{A}^3\mathcal{F} - \frac{1}{10}\mathcal{A}^5 \right) \ , \tag{52}$$

The exact instanton solutions in warped x^M space are not known. Some generic properties of these solutions can be inferred from large λ whatever the curvature. Indeed, since $\kappa \sim \lambda$, the instanton solution with unit topological charge that solves the full equations of motion, follows from the YM part only in leading order. It has zero size at infinite λ. At finite λ the instanton size is of order $1/\sqrt{\lambda}$. The reason is that while the CS contribution of order λ^0 is repulsive and wants the instanton to inflate, the warping in the z-direction of order λ^0 is attractive and wants the instanton to deflate in the z-direction [2, 3].

These observations suggest to use the flat space instanton configurations to leading order in $N_c\lambda$, with $1/\lambda$ corrections sought in perturbation theory. The latter is best achieved by rescaling the coordinates and the instanton fields as

$$\begin{aligned} x^M &= \lambda^{-1/2}\widetilde{x}^M \ , \quad x^0 = \widetilde{x}^0 \ , \\ \mathcal{A}_M &= \lambda^{1/2}\widetilde{\mathcal{A}}_M \ , \quad \mathcal{A}_0 = \widetilde{\mathcal{A}}_0 \ , \\ \mathcal{F}_{MN} &= \lambda\widetilde{\mathcal{F}}_{MN} \ , \quad \mathcal{F}_{0M} = \lambda^{1/2}\widetilde{\mathcal{F}}_{0M} \ . \end{aligned} \tag{53}$$

The corresponding energy density associated to the action (50) reads [3]

$$E = 8\pi^2\kappa\left[\frac{1}{16\pi^2}\int d^3\widetilde{x}d\widetilde{z}\mathrm{tr}\,\widetilde{F}^2_{MN}\right]$$
$$+\frac{\kappa}{\lambda}\int d^3\widetilde{x}d\widetilde{z}\left[-\frac{\widetilde{z}^2}{6}\mathrm{tr}\,\widetilde{F}^2_{ij}+\widetilde{z}^2\mathrm{tr}\,\widetilde{F}^2_{iz}-\frac{1}{2}(\widetilde{\partial}_M\widehat{\widetilde{A}}_0)^2-\frac{1}{32\pi^2 a}\widehat{\widetilde{A}}_0\mathrm{tr}\,\widetilde{F}^2_{MN}\right]\ . \tag{54}$$

All quantities are dimensionless in units of M_{KK}. The U(1) contribution $\widehat{\widetilde{A}}_0$ follows from the equation of motion [3]

$$\widetilde{\Box}\widehat{\widetilde{A}}_0 = \frac{1}{32\pi^2 a}\mathrm{tr}\,\widetilde{F}^2_{MN}\ . \tag{55}$$

The $\widehat{\widetilde{A}}_0$ field can be obtained in closed form using (11),

$$\widehat{\widetilde{A}}_0 = \frac{1}{32\pi^2 a}\widetilde{\Box}\log|f|\ . \tag{56}$$

According to (53) *both* the size of the instanton ρ and the distance d between two instantons are rescaled, i.e. $\widetilde{\rho}=\sqrt{\lambda}\rho$ and $\widetilde{d}=\sqrt{\lambda}d$. While the size $\widetilde{\rho}$ is fixed to $\widetilde{\rho}_0$ (see below) by the energy minimization process, the distance is not. Therefore, when discussing the energy at the subleading order, the distance $\widetilde{d}$ is always short for $\sqrt{\lambda}d$. It will be recalled whenever appropriate. The first term in (54) is $8\pi^2\kappa\times$ instanton number, which is identified with the bare soliton mass. The second term ($\equiv\Delta E$) is subleading and corresponds to the correction to the mass or the interaction energy

$$\begin{aligned}\Delta E &= \frac{\kappa}{\lambda}\int d^3\widetilde{x}d\widetilde{z}\left[-\frac{\widetilde{z}^2}{6}\mathrm{tr}\,\widetilde{F}^2_{ij}+\widetilde{z}^2\mathrm{tr}\,\widetilde{F}^2_{iz}-\frac{1}{2}(\widetilde{\partial}_M\widehat{\widetilde{A}}_0)^2-\frac{1}{32\pi^2 a}\widehat{\widetilde{A}}_0\mathrm{tr}\,\widetilde{F}^2_{MN}\right]\\ &= \frac{\kappa}{6\lambda}\int d^3\widetilde{x}d\widetilde{z}\left(\widetilde{z}^2-\frac{3^7\pi^2}{2^4}\widetilde{\Box}\log|f|\right)\widetilde{\Box}^2\log|f|\ ,\end{aligned} \tag{57}$$

where we used the self-duality, $\mathrm{tr}\,\widetilde{F}^2_{ij}=2\mathrm{tr}\,\widetilde{F}^2_{iz}=\frac{1}{2}\mathrm{tr}\,\widetilde{F}^2_{MN}$, and integrated $(\partial_M\widehat{\widetilde{A}}_0)^2$ by part so that it can be reduced to the form $\widehat{\widetilde{A}}_0\mathrm{tr}\,\widetilde{F}^2_{MN}$.

3.1 One baryon

The one baryon solution is the $k=1$ instanton. From (13) it follows that

$$f^{-1} = \widetilde{\rho}^2 + \widetilde{x}_M^2 \ , \tag{58}$$

for $k=1$. We have set $\widetilde{X}_i = 0$ by translational symmetry. We have also set $\widetilde{X}_4 = 0$ as a finite $\widetilde{X}_4$ cots energy [3]. Thus

$$\begin{aligned} \widetilde{\Box} \log f &= -4\frac{\widetilde{x}_M^2 + 2\widetilde{\rho}^2}{(\widetilde{x}_M^2 + \widetilde{\rho}^2)^2} \ , & (59) \\ \widetilde{\Box}^2 \log f &= \frac{96\widetilde{\rho}^4}{(\widetilde{x}_M^2 + \widetilde{\rho}^2)^4} \ . & (60) \end{aligned}$$

The mass correction $\Delta M \equiv \Delta E$, reads

$$\begin{aligned} \Delta M(\rho) &= \frac{\kappa}{6\lambda}\int d^3\widetilde{x}d\widetilde{z}\left(\widetilde{z}^2 + \frac{3^7\pi^2}{4}\frac{\widetilde{x}_M^2 + 2\widetilde{\rho}^2}{(\widetilde{x}_M^2 + \widetilde{\rho}^2)^2}\right)\frac{96\widetilde{\rho}^4}{(\widetilde{x}_M^2 + \widetilde{\rho}^2)^4} & (61) \\ &= \frac{8\pi^2\kappa}{\lambda}\left(\frac{\widetilde{\rho}^2}{6} + \frac{1}{320\pi^4 a^2}\frac{1}{\widetilde{\rho}^2}\right) \ . & (62) \end{aligned}$$

It depends on the size $\widetilde{\rho}$ as plotted in Fig. 1. All integrals in ΔM are analytical, since $\widetilde{\Box}\log|f|$ and $\widetilde{\Box}^2\log|f|$ are simple. For $k=2$ the expressions for ΔM are more involved and require numerical unwinding. As a prelude to these numerics, we have carried the integrals in (61) both analytically and numerically as illustrated in Fig.1.

The one-instanton stabilizes for

$$\widetilde{\rho}_0 = \sqrt{\frac{1}{8\pi^2 a}\sqrt{\frac{6}{5}}} \sim 9.64 \ , \tag{63}$$

with a mass correction

$$\Delta M(\widetilde{\rho}_0 \sim 9.64) \sim 0.365 \ . \tag{64}$$

We recall that the physical instanton size $\rho_0 = \widetilde{\rho}_0/\sqrt{\lambda}$ following the unscaling as detailed above.

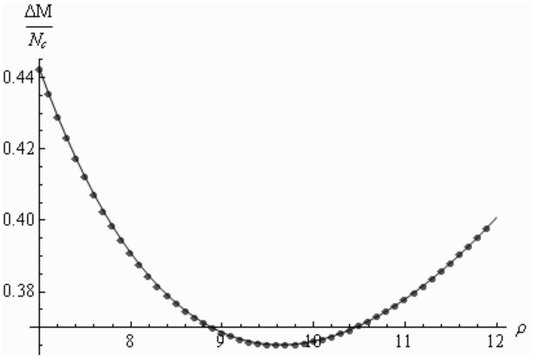

Figure 1: $\Delta M/N_c$: solid (exact) and dotted (numerical).

3.2 Two baryon

The two baryon solution corresponds to the $k=2$ instanton. The corresponding potential f for the $k=2$ instanton is given in (33) and yields

$$\begin{aligned}
\mathrm{tr}\,\widetilde{F}^2_{\mu\nu} &= \widetilde{\Box}^2 \log|f| \\
&= -\widetilde{\Box}^2 \log\Bigg[\left(g_-(\widetilde{x}_M) + \frac{\widetilde{\rho}_1^2\widetilde{\rho}_2^2 \sin^2|\,\theta|}{\widetilde{d}^2}\right)\left(g_+(\widetilde{x}_M) + \frac{\widetilde{\rho}_1^2\widetilde{\rho}_2^2 \sin^2|\,\theta|}{\widetilde{d}^2}\right) \\
&\qquad -\widetilde{\rho}_1^2\widetilde{\rho}_2^2\left(\cos|\,\theta| + \frac{2}{\widetilde{d}}\sin|\,\theta|\left[\widehat{\theta}_1\widetilde{x}_0 + \widehat{\theta}_2\widetilde{x}_3 - \widehat{\theta}_3\widetilde{x}_2\right]\right)^2\Bigg] \ . \qquad (65)
\end{aligned}$$

Its leading contribution in (54) is

$$8\pi^2\kappa\left[\frac{1}{16\pi^2}\int d^3\widetilde{x}d\widetilde{z}\mathrm{tr}\,\widetilde{F}^2_{MN}\right] = 2\times 8\pi^2\kappa \ ,$$

as expected by self-duality. To order $N_c\lambda$ the energy of the 2-baryon system is just $2M_0$ or twice the bare soliton mass. There is complete degeneracy in the moduli parameters $\widetilde{d}$ and θ_a. This degeneracy is lifted at order $N_c\lambda^0$, which is the next contribution in (54). This will be detailed below.

For two parallel instantons $|\,\theta| = 0$ and the instanton action density (65) reads

$$\mathrm{tr}\,\widetilde{F}^2_{\mu\nu} = -\widetilde{\Box}^2 \log\left[g_-(\widetilde{x}_M)g_+(\widetilde{x}_M) - \widetilde{\rho}_1^2\widetilde{\rho}_2^2\right] \ . \qquad (66)$$

The baryon number distribution in space follows from

$$B(x) = \frac{1}{16\pi^2}\int_{-\infty}^{+\infty} dz\,\mathrm{tr}\,F^2_{\mu\nu} \ , \qquad (67)$$

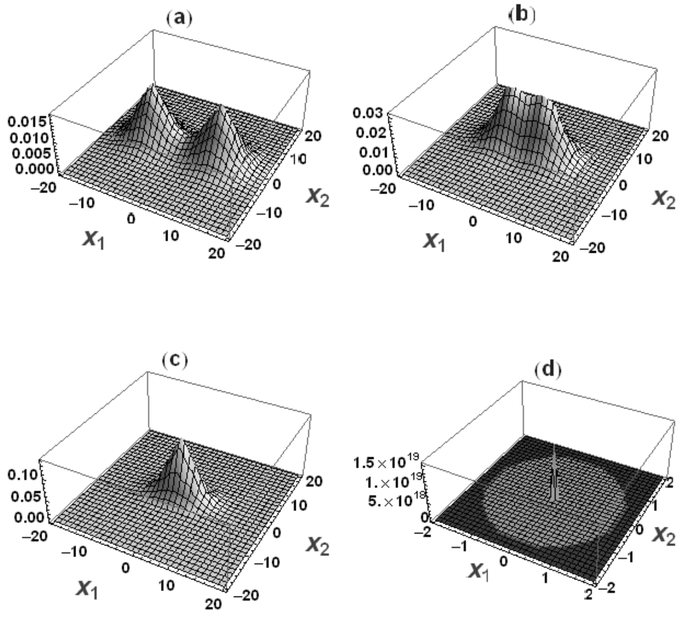

Figure 2: Defensive Skyrmions: (a) $\widetilde{d} = 2$, (b) $\widetilde{d} = \sqrt{2}$, (c) $\widetilde{d} = 1$, (d) $\widetilde{d} = 10^{-5}$

which integrates to 2. Since the instanton in bulk is localized near $z \approx \rho \approx 1/\sqrt{\lambda}$, we may approximate the integral by the value of the integrand for $z \approx 0$, or $B(x) \approx \mathrm{tr}\,\widetilde{F}^2_{\mu\nu}(z \approx 0)/16\pi^2$. In Fig. 2 we show $\mathrm{tr}\,\widetilde{F}^2_{\mu\nu}$ for $\widetilde{z} = \widetilde{x}_3 = 0$ and $\widetilde{\rho}_1 = \widetilde{\rho}_2 = 9.64$ for various separations $\widetilde{d}$ in the $(\widetilde{x}_1, \widetilde{x}_2)$ space for two paralell Skyrmions. The separation is in units of the size $\widetilde{\rho}_0 = 9.64$. For small separations a narrow Skyrmion develops on top of the broad Skyrmion. The configuration is maximally repulsive (defensive Skyrmions).

A paralell and antiparalell Skyrmion (combed Skyrmions) corresponds to the choice $\theta_1 = \theta_2 = 0$ and $\theta_3 = \frac{\pi}{2}$ or $|\,\theta| = \pi/2$. This is a π rotation along x_3 in the SO(3) notation (27). The resulting instanton action density (65) reads

$$\mathrm{tr}\,\widetilde{F}^2_{\mu\nu} \quad = \quad -\widetilde{\Box}^2 \log \left[\left(g_-(\widetilde{x}_M) + \frac{\widetilde{\rho}_1^2 \widetilde{\rho}_2^2}{\widetilde{d}^2} \right) \left(g_+(\widetilde{x}_M) + \frac{\widetilde{\rho}_1^2 \widetilde{\rho}_2^2}{\widetilde{d}^2} \right) - 4 \frac{\widetilde{\rho}_1^2 \widetilde{\rho}_2^2}{\widetilde{d}^2} \widetilde{x}_2^2 \right] . \qquad (68)$$

In Fig. 3 we show the baryon density in the plane (x_1, x_2) for various separations in units of the instanton size with $\widetilde{\rho}_1 = \widetilde{\rho}_2 = 9.64$. For large separation two lumps form along the x^1 axis. For smaller separation the two lumps are seen to form in the orthogonal or x_2 direction. In between a hollow baryon 2 configuration is seen which is the precursor of the donut seen in the baryon number 2 sector of the Skyrme model [19]. The concept of $\widetilde{d}$ as a separation at small separations is no longer physical given the separation taking place in the transverse direction. What is physical is the dual distance u in the transverse plane.

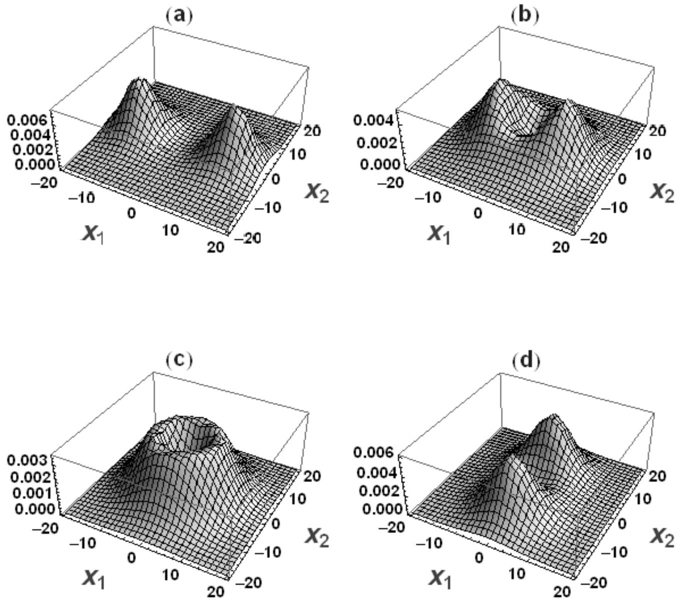

Figure 3: Combed Skyrmions: (a) $\widetilde{d} = 2.5$, (b) $\widetilde{d} = 1.7$, (c) $\widetilde{d} = \sqrt{2}$, (d) $\widetilde{d} = 1$

For two Skyrmions orthogonal to each other, the choice of angles is $\theta_1 = \theta_2 = 0, \theta_3 = \frac{\pi}{4}$. The corresponding action density is given by (65)

$$\begin{aligned} \mathrm{tr}\, \widetilde{F}_{\mu\nu}^2 &= -\widetilde{\Box}^2 \log \Bigg[\left(g_-(\widetilde{x}_M) + \frac{\widetilde{\rho}_1^2 \widetilde{\rho}_2^2 \sin^2\theta_3}{\widetilde{d}^2} \right) \left(g_+(\widetilde{x}_M) + \widetilde{\rho}_2^2 + \frac{\widetilde{\rho}_1^2 \widetilde{\rho}_2^2 \sin^2\theta_3}{\widetilde{d}^2} \right) \\ &\qquad - \widetilde{\rho}_1^2 \widetilde{\rho}_2^2 \left(\cos\theta_3 - \frac{2\widetilde{x}_2}{\widetilde{d}} \sin\theta_3 \right)^2 \Bigg] \ , \end{aligned} \tag{69}$$

which is also seen to reduce to (66) and (68) for $\theta_3 = 0$ or π and $\theta_3 = \pi/2$ respectively. The $\theta_3 = \frac{\pi}{4}$ is our two orthogonal Skyrmions. This configuration is shown in Fig.(4). For small separations a narrow Skyrmion develops on top of a broad one, a situation reminiscent of the Defensive Skyrmion configuration above. This situation can be seen in many other relative orientations and is somehow generic.

4 Skyrmion-Skyrmion Interaction

The Skyrmion-Skyrmion interaction in hQCD is of order N_c/λ and it follows from (57) which is the second term in (54). The baryon two minimum energy configuration should follow by minimizing this contribution in the 6-dimensional coset space ρ, d, θ. This will be reported elsewhere. Instead, we report on the interaction energy between two Skyrmions versus their

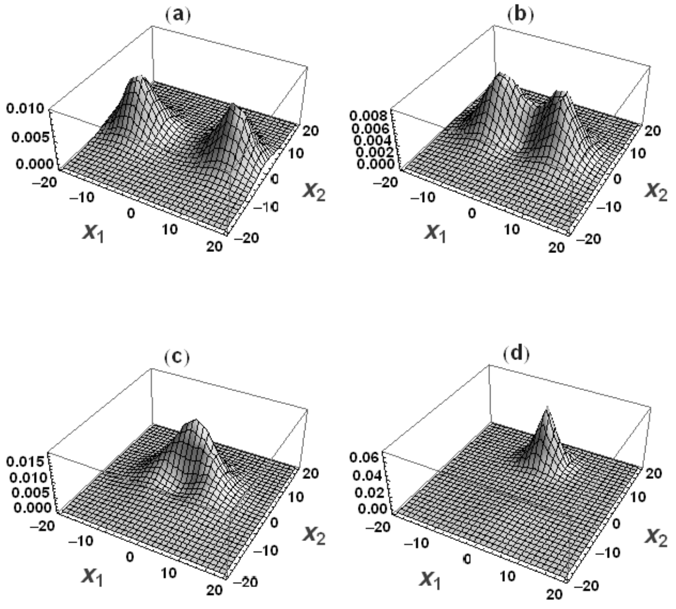

Figure 4: Orthogonal Skyrmions: (a) $\widetilde{d} = 2.5$, (b) $\widetilde{d} = 1.7$, (c) $\widetilde{d} = 1.2$, (d) $\widetilde{d} = 0.6$.

separation for a size fixed in the baryon 1 sector and different relative orientations θ_a. In the adiabatic quantization scheme, θ_a are raised to collective coordinates. They are not fixed by minimization. This approach will be subsumed here. We note that the mass shift are of order $N_c\lambda^0$.

4.1 General

Consider the case where $\theta_1 = \theta_2 = 0$ and $\theta_3 \neq 0$, with fixed sizes $\widetilde{\rho}_1 = \widetilde{\rho}_2 = \widetilde{\rho}_0$. Here $\widetilde{\rho}_0$ is the value fixed by minimization in the 1 Skyrmion sector (63). In Fig. (5) we show the interaction energy $(\Delta E - 2\Delta M)/N_c$ versus the relative distance d in units of the instanton size, where

$$\Delta E = \frac{\kappa}{6\lambda}\int d^3\widetilde{x}\, d\widetilde{z}\left(\widetilde{z}^2 - \frac{3^7\pi^2}{2^4}\widetilde{\Box}\log|f|\right)\widetilde{\Box}^2\log|f| \ , \tag{70}$$

$$\begin{aligned} |f| = &\left(g_-(\widetilde{x}_M) + \frac{\widetilde{\rho}_1^2\widetilde{\rho}_2^2\sin^2\theta_3}{\widetilde{d}^2}\right)\left(g_+(\widetilde{x}_M) + \frac{\widetilde{\rho}_1^2\widetilde{\rho}_2^2\sin^2\theta_3}{\widetilde{d}^2}\right) \\ &-\widetilde{\rho}_1^2\widetilde{\rho}_2^2\left(\cos\theta_3 - \frac{2\widetilde{x}_2}{\widetilde{d}}\sin\theta_3\right)^2 \ . \end{aligned} \tag{71}$$

The interaction energy is repulsive for all values of θ_3. The repulsion decreases for θ_3 in the range $0 \to \pi/2$, that is from the defensive to combed configuration. The defensive or

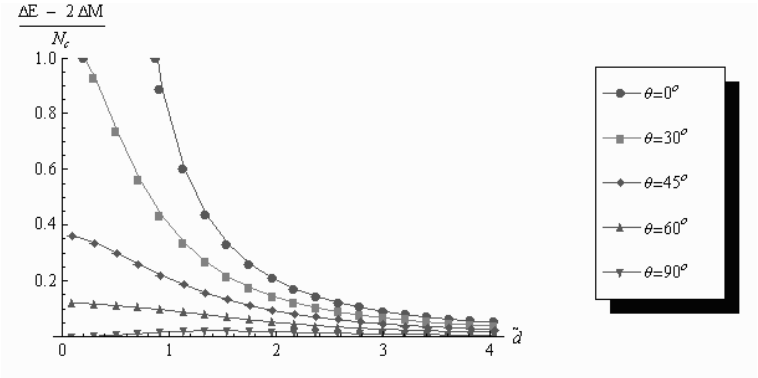

Figure 5: Skyrmion-Skyrmion interaction in regular gauge.

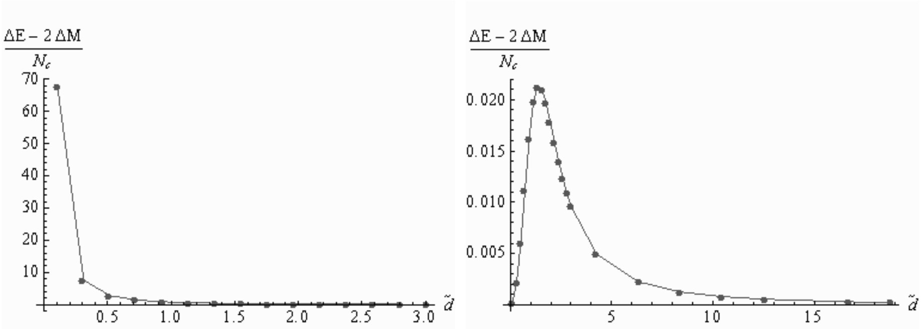

Figure 6: Skyrmion-Skyrmion interaction: Defensive (left) and Combed (right)

$\theta_3 = \pi/2$ is still repulsive even for small relative distances, as the two Skyrmions separate in the transverse direction. In Fig. (6) we show separatly the interaction energy for the defensive configuration (left) and combed configuration (right). The repulsion is seen to drop by 3 orders of magnitude.

The core interaction is modified in the singular gauge as we detail in Appendix A and B. In Fig. (7) we show the analogue of Fig. (5) in the singular gauge. The switch from repulsion to attraction follows from the switch from repulsive Coulomb (regular gauge) to attractive dipole (singular gauge) interactions. The plot is versus $\tilde{d}$ which is the rescaled distance in units of the rescaled size $\tilde{\rho}$. In the unscaled distance d, the dipole attraction is of order N_c/λ^4 and subleading.

4.2 Interaction at Large Separation

To understand the nature of the Skyrmion-Skyrmion interaction to order N_c/λ as given by the classical instantons in bulk, we now detail it for large separations between the instanton

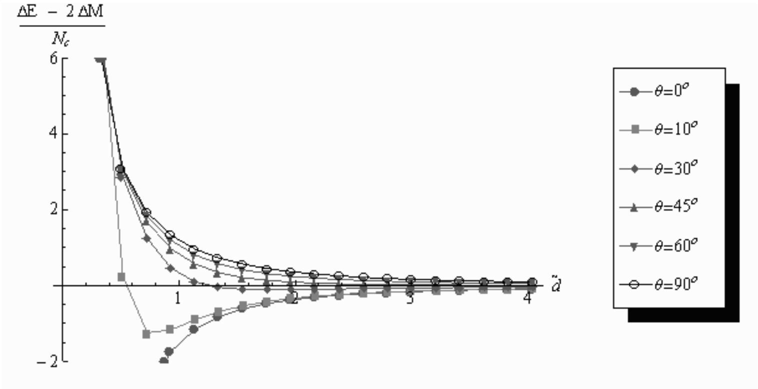

Figure 7: Skyrmion-Skyrmion interaction in singular gauge

cores, i.e. $d \gg \rho$ but still smaller than the pion range (which is infinite for massless pions). We recall that the interaction follows from the subleading contribution in (54), which can be split

$$
\begin{aligned}
\Delta E[f] &= N_c b\,(C[f] + c\,D[f])\ , & (72)\\
C[f] &\equiv \int d^3\widetilde{x} d\widetilde{z}\, \widetilde{z}^2\, \widetilde{\Box}^2 \log|f|\ , & (73)\\
D[f] &\equiv -\int d^3\widetilde{x} d\widetilde{z}\, (\,\widetilde{\Box}^2 \log|f|\,)\, \frac{1}{\widetilde{\Box}}\, (\,\widetilde{\Box}^2 \log|f|\,)\ , & (74)
\end{aligned}
$$

with $b = \frac{1}{6\cdot 216\pi^3}$ and $c \equiv \frac{3^7\pi^2}{2^4}$.

For large separations between the cores or $d \gg \rho$, we have from (37)

$$
\begin{aligned}
\log|f_{-+}| &= -\log\left[(g_- g_+)\left(1 + A\frac{g_- + g_+}{g_- g_+} + \frac{A^2 - B^2}{g_- g_+}\right)\right]\\
&\approx -\log g_- - \log g_+ - A\frac{g_- + g_+}{g_- g_+} + \frac{B^2}{g_- g_+}\ , \qquad (75)
\end{aligned}
$$

after dropping the A^2 contribution as it is subleading in ρ/d. We note that after fixing the size of the single instanton to $\widetilde{\rho}_0$ and *unscaling* the distance $\widetilde{d}$ as we indicated above, the expansion $\widetilde{\rho}/\widetilde{d}$ is an expansion in $\widetilde{\rho}_0/(\sqrt{\lambda} d)$.

The Skyrmion-Skyrmion core interaction follows from

$$
V = \Delta E[f_{-+}] - \Delta E[f_-] - \Delta E[f_+]\ , \qquad (76)
$$

after subtraction of the classical self-energies which are of order $N_c\lambda^0$. The $C[f]$ contribution to the interaction reads

$$V_C = \sin^2|\,\theta|\,V_{C\alpha} + \sin^2|\,\theta|\,\widehat{\theta}_1^2 V_{C\beta} + \sin^2|\,\theta|\,(\widehat{\theta}_2^2+\widehat{\theta}_3^2)V_{C\gamma} + \cos^2|\,\theta|\,V_{C\delta}\ , \tag{77}$$

with

$$\begin{aligned}
V_{C\alpha} &\equiv N_c b\frac{\widetilde{\rho}^4}{\widetilde{d}^2}\int d^3\widetilde{x}d\widetilde{z}\,\widetilde{z}^2\,\widetilde{\Box}^2\left(\frac{g_-+g_+}{g_-g_+}\right)\ , &(78)\\
V_{C\beta} &\equiv N_c b\frac{\widetilde{\rho}^4}{\widetilde{d}^2}\int d^3\widetilde{x}d\widetilde{z}\,\widetilde{z}^2\,\widetilde{\Box}^2\left(\frac{4\widetilde{z}^2}{g_-g_+}\right)\ , &(79)\\
V_{C\gamma} &\equiv N_c b\frac{\widetilde{\rho}^4}{\widetilde{d}^2}\int d^3\widetilde{x}d\widetilde{z}\,\widetilde{z}^2\,\widetilde{\Box}^2\left(\frac{4\widetilde{x}_2^2}{g_-g_+}\right)\ , &(80)\\
V_{C\delta} &\equiv N_c b\frac{\widetilde{\rho}^4}{\widetilde{d}^2}\int d^3\widetilde{x}d\widetilde{z}\,\widetilde{z}^2\,\widetilde{\Box}^2\left(\frac{1}{g_-g_+}\right)\ , &(81)
\end{aligned}$$

where the cross term in B^2 drops by parity and we have rescaled the variable $\widetilde{x}_M/\widetilde{d} \to \widetilde{x}_M$. Thus $g_\pm \to \widetilde{x}_\alpha^2 + \left(\widetilde{x}_1 \pm \frac{1}{2}\right)^2 + \widetilde{\rho}^2/\widetilde{d}^2$. All integrals are understood in dimensional regularization that preserves both gauge and $O(4)$ symmetry. The results are

$$V_{C\alpha} = -V_{C\beta} = -V_{C\gamma} = N_c b\frac{\widetilde{\rho}^4}{\widetilde{d}^2}16\pi^2\ , \qquad V_{C\delta} = 0\ . \tag{82}$$

The $D[f]$ contribution to the interaction reads

$$V_D \approx -2bcN_c\int(\,\widetilde{\Box}^2\log g_-\,)\,\frac{1}{\widetilde{\Box}}\,(\,\widetilde{\Box}^2\log g_+\,)\ . \tag{83}$$

The Coulomb propagator $1/\widetilde{\Box} = -1/(4\pi^2|\widetilde{x}_+ - \widetilde{x}_-|^2)$ in 4-dimensions. At large separations $|\widetilde{x}_+ - \widetilde{x}_-| \approx \widetilde{d}$ and (83) simplifies to

$$V_D \approx 128\pi^2\,bcN_c\frac{1}{d^2}\left|\frac{1}{16\pi^2}\int d^3\widetilde{x}d\widetilde{z}\,\widetilde{\Box}^2\log g\right|^2 = \frac{27\pi N_c}{2}\frac{1}{\widetilde{d}^2}\ , \tag{84}$$

where the $||$ integrates to the baryon charge 1. V_D captures the Coulomb repulsion between two unit baryons in 4 dimensions in the regular gauge. This is not the case in the singular as we show in Appendix B.

We note that after unscaling $\widetilde{d} = \sqrt{\lambda}d$, $V_D \approx N_c/\lambda$. In regular gauge, this monopole core repulsion is the Coulomb repulsion between *4-dimensional* Coulomb charges. We show in Appendix C that this is the natural extension of the *3-dimensional* omega repulsion at shorter distances in holography. The repulsion dominates the many-body problem at finite chemical potential as discussed recently in [4, 5]. Indeed, for baryonic matter at large baryonic density n_B, the energy is dominated by the Coulomb repulsion (84). The corresponding effective interaction is

$$V_{\rm eff} = \frac{1}{2}\int d\vec{x}d\vec{y}\left(\phi^+\phi\right)(\vec{x})V_D(\vec{x}-\vec{y})\left(\phi^+\phi\right)(\vec{y}) \ , \tag{85}$$

leading to an energy per volume of order $N_c\, n_B^{5/3}/\lambda$ as in [5].

5 Nucleon-Nucleon Interaction: Core

At large separation, the nucleon-nucleon core interaction can be readily extracted from the Skyrmion-Skyrmion core interaction (77) as it is linear in the $SO(3)$ rotation R. Indeed, using the standard decomposition [14]

$$R^{ab} = \frac{1}{3}(R_T^{ab} + \delta^{ab}R_S) \ , \tag{86}$$

with

$$R_S = {\rm tr}\, R \ , \quad R_T^{ab} = 3R^{ab} - \delta^{ab}{\rm tr}\, R \ , \tag{87}$$

the spin R_S and tensor R_T contributions respectively, we may decompose the core potential as

$$V = V_1 + V_S R_S + V_T^{ab}R_T^{ab} \ . \tag{88}$$

The scalar V_1, spin V_S and tensor V_T contributions can be unfolded by a pertinent choice of orientations of the core Skyrmion-Skyrmion interaction. In general,

$$V = V_1 + V_S\left(4\cos^2|\,\theta| - 1\right) + V_T^{ab}\left[\left(6\hat{\theta}^a\hat{\theta}^b - 2\delta^{ab}\right)\sin^2|\,\theta| + 3\epsilon^{abc}\widehat{\theta}^c\sin 2|\,\theta|\right] \ , \tag{89}$$

after using the SO(3) parametrization (27)

$$R^{ab} = \delta^{ab}\cos 2|\,\theta| + 2\widehat{\theta}^a\widehat{\theta}^b\sin^2|\,\theta| + \epsilon^{abc}\widehat{\theta}^c\sin 2|\,\theta| \ . \tag{90}$$

The axial symmetry $V(\theta_1,\theta_2,\theta_3) = V(\theta_1,\theta_3,\theta_2)$ implies that the tensor components of the core satisfy $V_T^{22} = V_T^{33}, V_T^{12} = V_T^{31}$, and $V_T^{13} = V_T^{21}$. Thus, V is reduced to

$$
\begin{aligned}
V(\theta_1,\theta_2,\theta_3) &= V_1 + V_S\left(4\cos^2|\,\theta| - 1\right) + (V_T^{11} - V_T^{22})(6\hat{\theta}_1^2 - 2)\sin^2|\,\theta| \\
&+ (V_T^{12} + V_T^{13})(6\hat{\theta}_1(\hat{\theta}_2 + \hat{\theta}_3))\sin^2|\,\theta|) + (V_T^{12} - V_T^{13})(3(\hat{\theta}_2 + \hat{\theta}_3)\sin 2|\,\theta|) \\
&+ (V_T^{23} + V_T^{32})(6\hat{\theta}_2\hat{\theta}_3\sin^2|\,\theta|) + (V_T^{23} - V_T^{32})(3\hat{\theta}_1\sin 2|\,\theta|)\ . \qquad (91)
\end{aligned}
$$

In particular,

$$
\begin{aligned}
&V(0,0,0) = V_1 + 3V_S\ , \quad V(0,0,\pi/2) = V_1 - V_S - 2(V_T^{11} - V_T^{22})\ , \qquad (92) \\
&V(\pi/2,0,0) = V_1 - V_S + 4(V_T^{11} - V_T^{22})\ , \qquad (93)
\end{aligned}
$$

so that

$$
\begin{aligned}
V_1 &= \frac{1}{4}\left[V(0,0,0) + V(0,0,\pi/2) + V(0,\pi/2,0) + V(\pi/2,0,0)\right]\ , \qquad (94) \\
V_S &= \frac{1}{4}\left[V(0,0,0) - \frac{1}{3}\left(V(0,0,\pi/2) + V(0,\pi/2,0) + V(\pi/2,0,0)\right)\right]\ , \qquad (95) \\
V_T^{11} - V_T^{22} &= \frac{1}{6}\left[V(\pi/2,0,0) - V(0,0,\pi/2)\right]\ . \qquad (96)
\end{aligned}
$$

Using (78)-(81) we deduce the scalar, spin and tensor core contributions in the form

$$
\begin{aligned}
V_1 &= \frac{1}{4}\left(3V_{C\alpha} + V_{C\beta} + 2V_{C\gamma} + V_{C\delta}\right) + V_D = V_D\ , \\
V_S &= \frac{1}{4}\left(-V_{C\alpha} - \frac{1}{3}V_{C\beta} - \frac{2}{3}V_{C\gamma} + V_{C\delta}\right) = 0\ , \\
V_T^{11} - V_T^{22} &= \frac{1}{6}(V_{C\beta} - V_{C\gamma}) = 0\ . \qquad (97)
\end{aligned}
$$

The off-diagonal tensor V_T core contribution vanishes. This is clear from (77). Indeed (77) can be decomposed as

$$
\begin{aligned}
V &= \sin^2|\,\theta|\,V_{C\alpha} + \sin^2|\,\theta|\,\widehat{\theta}_1^2 V_{C\beta} + \sin^2|\,\theta|\,(\widehat{\theta}_2^2 + \widehat{\theta}_3^2)V_{C\gamma} + \cos^2|\,\theta|\,V_{C\delta} + V_D \\
&= \sin^2|\,\theta|\,(V_{C\alpha} + V_{C\gamma}) + \sin^2|\,\theta|\,\widehat{\theta}_1^2(V_{C\beta} - V_{C\gamma}) + \cos^2|\,\theta|\,V_{C\delta} + V_D \\
&= \frac{1}{4}\left(3V_{C\alpha} + V_{C\beta} + 2V_{C\gamma} + V_{C\delta}\right) + V_D \\
&\quad + \frac{1}{4}\left(-V_{C\alpha} - \frac{1}{3}V_{C\beta} - \frac{2}{3}V_{C\gamma} + V_{C\delta}\right)\left(4\cos^2|\,\theta| - 1\right) \\
&\quad + \frac{1}{6}(V_{C\beta} - V_{C\gamma})(6\hat{\theta}_1^2 - 2)\sin^2|\,\theta|\ , \qquad (98)
\end{aligned}
$$

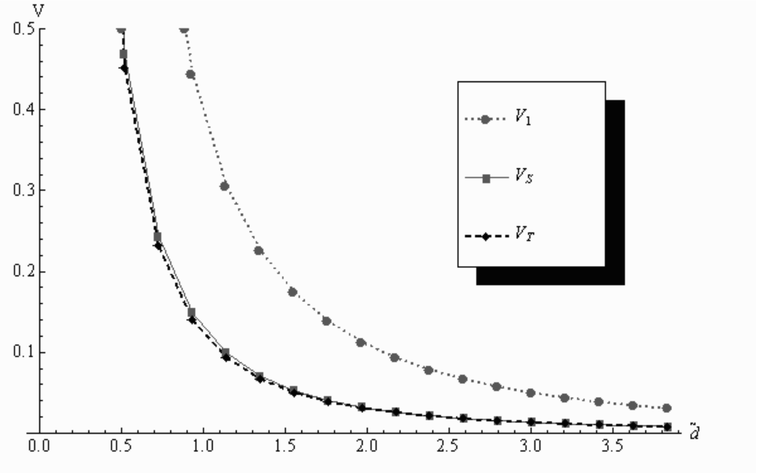

Figure 8: V_1, V_S, V_T in regular gauge

in agreement with (97). In summary

$$V_1 = V_D \ , \tag{99}$$

and all others vanish. For general distances, we plot V_1, V_S and V_T with (94)-(96) in Fig.(8) in the regular gauge. The relative separation $\tilde{d}$ is in units of the core size $\tilde{\rho} = 9.64$.

In the singular gauge, the V_C core contribution to the nucleon-nucleon interaction remains unchanged while the V_D contribution changes. As a result, the spin and tensor channels remain the same for both regular and singular gauges. The central or scalar channel $V_1 = V_D$ changes from repulsive $N_c/\lambda\widetilde{d}^2$ (regular) to attractive $-N_c/\lambda^4\widetilde{d}^8$ (singular) asymptotically. The flip is from monopole to dipole as we detail in Appendix B. The short distance repulsion in the regular gauge is the 4-dimensional extension of the 3-dimensional omega repulsion. In Fig.(9) we show V_1, V_S and V_T with (94)-(96) and (158) in the singular gauge.

6 Nucleon-Nucleon Interaction: Cloud

To assess the nucleon-nucleon interaction beyond the core contribution we need to do a semiclassical expansion around the $k = 2$ configuration, thereby including the effects of pions and vector mesons as quantum fluctuations around the core. We refer to these contributions as the cloud. The semiclassical expansion around the $k = 2$ configuration parallells entirely the same expansion around the $k = 1$ instanton as detailed in [7]. The expansion will be carried out in the axial gauge $A_z = 0$ for the fluctuations. This gauge has the merit of

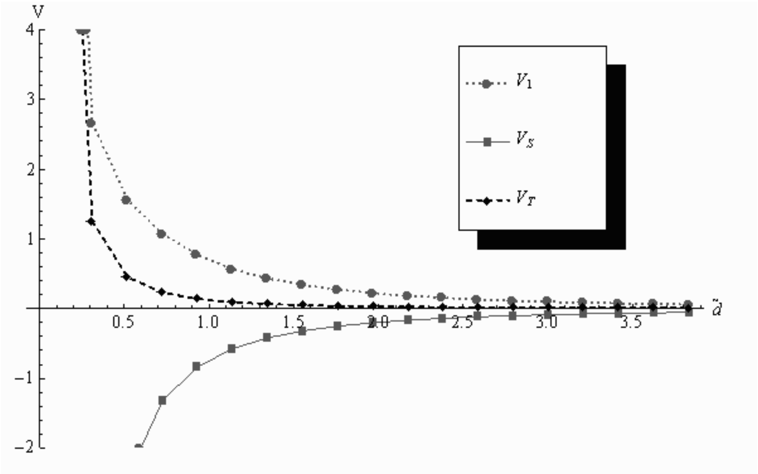

Figure 9: V_1, V_S, V_T in singular gauge

exposing explicitly the pion-nucleon coupling. All cloud calculations will be carried with the background $k = 2$ instanton in the regular gauge. Some of the results in the singular gauge are reported in Appendix C.

6.1 Pion

In the axial gauge $A_z = 0$ for the fluctuations, the pion coupling to the flavor instanton is explicit in bulk. Indeed, following the general expansion in [7] we have for the pion-instanton linear coupling

$$S = -\kappa \int d^4x dz \partial_z \left(K F^a_{z\mu} C^{\mu,a} \right) \ , \tag{100}$$

with the explicit pion field

$$C^{\mu,a} \equiv \frac{1}{f_\pi} \partial^\mu \Pi^a \psi_0 \ , \quad \psi_0 = \frac{2}{\pi} \arctan z \ , \tag{101}$$

and $f_\pi = 4\kappa/\pi$. As noted in [7] all linear meson couplings to the flavor instanton are boundary-like owing to the soliton character of the $k = 2$ instanton. Since $KF_{zi}\psi_0$ is odd in z, for a static instanton,

$$S = \kappa \int d^4x F^a_{zi} K \psi_0 \Big|_B \frac{\partial_i \Pi^a}{f_\pi} \ . \tag{102}$$

Here $B = \pm z_c$ refers to boundary of the core when using the non-rigid quantization scheme. To avoid double counting, for $z < z_c$ the mesons are excluded in the holographic direction. z_c plays the role of the bag radius. It will be reduced to $z_c \to 0$ at the end of all calculations, making the non-rigid quantization constraint point-like.

The linear pion-2-instanton vertex (102) contributes to the energy through second order perturbation. Specifically,

$$\begin{aligned} V_\Pi &= \frac{4\kappa^2 K(z_c)^2 \psi_0(z_c)^2}{2f_\pi^2} \int d\vec{x} d\vec{y} F^a_{iz}(\vec{x}, z_c) \langle \partial_i \Pi(\vec{x})^a \partial_j \Pi(\vec{y})^b \rangle F^b_{jz}(\vec{y}, z_c) && (103) \\ &= \frac{\kappa^2 K(z_c)^2 \psi_0(z_c)^2}{2\pi f_\pi^2} \int d\vec{x} d\vec{y} F^a_{iz}(\vec{x}, z_c) \partial_i \partial_j \frac{1}{|\vec{x} - \vec{y}|} F^a_{jz}(\vec{y}, z_c) \ , && (104) \end{aligned}$$

for massless pions. At large separations, the field strength F^a_{iz} splits into two single instantons of relative distance d and flavor orientation R. At large relative separation d, (104) simplifies to

$$V_\Pi \approx \frac{9}{16\pi f_\pi^2} J_A^{ai}(0) D_{ij} J_A^{Raj}(0) \ , \tag{105}$$

with $D_{ij} = (3\hat{d}_i \hat{d}_j - \delta_{ij})/d^3$. The spatial component of the axial vector current J_A is unrotated while J_A^R is rotated. From Appendix D, its zero momentum limit reads

$$J_A^{ai}(0) \equiv J_A^{ai}(\vec{q} = 0) = -\frac{4}{3} \kappa K(z_c) \psi_0(z_c) \int d\vec{x}\, F^a_{iz}(\vec{x}, z_c) \ . \tag{106}$$

The projected potential V_Π yields

$$\begin{aligned} \langle s_1 t_1 s_2 t_2 | V_\Pi | s_1 t_1 s_2 t_2 \rangle &= \frac{9}{16\pi f_\pi^2} \langle s_1 t_1 | J_A^{ai}(0) | s_1 t_1 \rangle D_{ij} \langle s_2 t_2 | J_A^{RAj}(0) | s_2 t_2 \rangle \\ &\equiv \frac{1}{16\pi} \left(\frac{g_A}{f_\pi} \right)^2 \frac{1}{d^3} \Big(3(\vec{\sigma}_1 \cdot \widehat{d})(\vec{\sigma}_2 \cdot \widehat{d}) - \vec{\sigma}_1 \cdot \vec{\sigma}_2 \Big) (\vec{\tau}_1 \cdot \vec{\tau}_2) \ , \end{aligned} \tag{107}$$

where $g_A = 32\kappa\pi\rho^2/3$ is the axial-vector charge of the nucleon as detailed in Appendix D. $g_A \approx N_c \lambda^0$ in hQCD.

In the $A_z = 0$ gauge, the linear pion-2-instanton vertex (100) yields a tensor contribution to the nucleon-nucleon potential

$$V_{T,\Pi} = \frac{1}{16\pi} \left(\frac{g_A}{f_\pi} \right)^2 \frac{1}{d^3} \ . \tag{108}$$

This is in agreement with the pseudo-vector one-pion exchange potential

$$V_{T,\Pi} = \frac{(g_{\pi NN}/2M)^2}{4\pi} \frac{1}{d^3} , \tag{109}$$

if we identify

$$\frac{g_{\pi NN}}{M_N} = \frac{g_A}{f_\pi} . \tag{110}$$

This is just the Goldberger-Treiman relation which is also satistified by the holographic construction in the $A_z = 0$ gauge and for massless pions.

In reaching (107) and the relation (110) there is a subtlety. Indeed in (105) the pion propagator D_{ij} is supposed to be longitudinal and the axial vector source J_A^{ij} transverse, so that the contraction vanishes. The subtlety arises from the ambiguity in the axial vector source at zero momentum and for massless pions as discussed in Appendix D. The contraction is ambiguous through 0/0. The ambiguity is lifted by the order of limits detailed in Appendix D, which effectively amounts to a longitudinal component of the axial vector source at zero momentum. This result is independently confirmed by using the strong coupling source theory discussed in Appendix C.

Finally, the pion coupling (102) in the axial gauge is pseudoscalar and strong and of order $\sqrt{N_c/\lambda}$. The reader may object that this conclusion maybe at odd with naive $1/N_c$ power counting whereby the pseudovector coupling is of order $\sqrt{N_c}/N_c \approx 1/\sqrt{N_c}$ with the extra $1/N_c$ suppression brought about by the γ_5 in the nucleon axial vector source [14]. In strongly coupled models such as hQCD the nucleon source is of order N_c^0 not $1/N_c$, and yet chiral symmetry is fully enforced in the nucleon sector. hQCD is a chiral and dynamical version of the static Chew model of the Δ for strong coupling [20]. Also, the reader may object that the one-pion iteration which is producing a potential of order N_c/λ, may cause an even stronger correction by double iteration of order $(N_c/\lambda)^{3/2}$ and so on. This does not happen though, since the direct and crossed diagram to order $(N_c/\lambda)^{3/2}$ cancel at strong coupling. The same cancellation is at the origin of unitarization in $\pi N \rightarrow \pi N$ scattering (Bhabha-Heithler mechanism).

6.2 Axials

The linear vertex (100) also couples vector and axial vector mesons to the 2-instanton solution at the core in bulk. For instance, the axial-vector meson contribution follows from (100) by inserting

$$C^{\mu,a} \equiv a_{\mu}^{a,n}\psi_{2n} \ , \tag{111}$$

so that

$$S = 2\kappa \int d^4x \left(K\mathbb{F}^{b,z\mu} a_{\mu}^{b,n}\psi_{2n}\right)\Big|_{z=z_c} \ . \tag{112}$$

The sum over n is subsumed. We have used the fact that $KF_{zi}\psi_{2n}$ is odd in z (axial exchange) and that the surface contribution at $z=\infty$ is zero since ${F^b}_{z\nu} \sim \delta(z)$ is localized in bulk to leading order in $1/\lambda$.

In second order perturbation, (112) contributes a static potential

$$V_A \ \ = \ \ 2\kappa^2 K(z_c)^2 \psi_{2n}(z_c)\psi_{2m}(z_c)\int d\vec{x}d\vec{y} F_{iz}^a(\vec{x},z_c)\Delta_{ij}^{mn,ab} F_{jz}^b(\vec{y},z_c) \ . \tag{113}$$

At large separations, the field strength F_{iz}^a splits into two single instantons of relative distance d and flavor orientation $R = R_1^T R_2$. At large relative separation d, (113) simplifies to [1]

$$\begin{aligned} V_A \ &\approx \ \frac{9}{16\pi}\sum_n J_A^{ai}(0)\left(\frac{\psi_{2n}}{\psi_0}\right)^2 \left(-\delta_{ij} + \frac{\partial_i\partial_j}{m_{2n}^2}\right)\frac{e^{-m_{2n}d}}{d} J_A^{Raj}(0) \\ &= \ \frac{9}{16\pi}\sum_n J_A^{ai}(0)\left(\frac{\psi_{2n}}{\psi_0}\right)^2 \left[\left(1+\frac{2}{m_{2n}d}+\frac{3}{m_{2n}^2 d^2}\right)\widehat{d}_i\widehat{d}_j \right. \\ &\qquad\qquad \left. -\delta_{ij}\left(1+\frac{1}{m_{2n}^2 d^2}\right)\right]\frac{e^{-m_{2n}d}}{d} J_A^{Raj}(0) \ , \end{aligned} \tag{114}$$

where $J_A^{ai}(0)$ is defined in (106) and the spatial component of the axial vector current J_A is unrotated while J_A^R is rotated. The projected potential V_A yields

$$\begin{aligned} &\langle s_1 t_1 s_2 t_2 | V_A | s_1 t_1 s_2 t_2\rangle \\ &\quad \approx \frac{g_A^2}{16\pi}\sum_n \left(\frac{\psi_{2n}}{\psi_0}\right)^2 e^{-m_{2n}d}\left(-\frac{1}{d}-\frac{1}{m_{2n}^2 d^3}\right)(\vec{\sigma}_1\cdot\vec{\sigma}_2)(\vec{\tau}_1\cdot\vec{\tau}_2) \\ &\quad\quad + \frac{g_A^2}{16\pi}\sum_n \left(\frac{\psi_{2n}}{\psi_0}\right)^2 e^{-m_{2n}d}\left(\frac{1}{d}+\frac{2}{m_{2n}d^2}+\frac{3}{m_{2n}^2 d^3}\right)(\vec{\sigma}_1\cdot\widehat{d})(\vec{\sigma}_2\cdot\widehat{d})(\vec{\tau}_1\cdot\vec{\tau}_2) \\ &\quad \approx \frac{g_A^2}{16\pi}\sum_n \left(\frac{\psi_{2n}}{\psi_0}\right)^2 \frac{e^{-m_{2n}d}}{d}\left[(\vec{\sigma}_1\cdot\widehat{d})(\vec{\sigma}_2\cdot\widehat{d}) - (\vec{\sigma}_1\cdot\vec{\sigma}_2)\right](\vec{\tau}_1\cdot\vec{\tau}_2) \ , \end{aligned} \tag{115}$$

---

[1] For simplicity we often omit $|_{z=z_c}$ and $\psi_n \equiv \psi_n(z_c)$.

which contributes to the spin $V_{S,A}$ and tensor part $V_{T,A}$ of the NN interaction. Specifically,

$$\begin{aligned}
&V_{S,A} \approx \sum_n G^2_{SA,2n} \frac{e^{-m_{2n}}d}{4\pi\, d} \ , \quad V_{T,A} \approx \sum_n G^2_{TA,2n} \frac{e^{-m_{2n}}d}{4\pi\, d} \ , \\
&G_{SA,2n} \equiv -\frac{g_A\psi_{2n}}{\sqrt{6}\psi_0} \sim g_A m_{2n}/\sqrt{\kappa} \ , \qquad G_{TA,2n} \equiv \frac{g_A\psi_{2n}}{\sqrt{12}\psi_0} \sim g_A m_{2n}/\sqrt{\kappa} \ , \qquad (116)
\end{aligned}$$

with $G_{SA,2n} \approx \sqrt{N_c/\lambda}$ and $G_{TA,2n} \approx \sqrt{N_c/\lambda}$ the spin and tensor couplings of the tower of axials to the nucleon.

6.3 Vectors

For the vector mesons the time component F_{0z} contribution is leading in N_c compared to the space component F_{iz}. This is the opposite of the axial vector contribution. For the SU(2) part (rho, rho', ...), we have

$$\begin{aligned}
V_V &= \frac{1}{2\pi} \sum_n \kappa^2 K(z_c)^2 \psi^2_{2n-1}(z_c) \int d\vec{x} d\vec{y} F^a_{0z}(\vec{x}, z_c) \frac{e^{-m_{2n-1}|\vec{x}-\vec{y}|}}{|\vec{x}-\vec{y}|} F^a_{0z}(\vec{y}, z_c) \\
&\approx \frac{1}{4\pi} \sum_n J^a \psi^2_{2n-1} \frac{e^{-m_{2n-1}d}}{d} J^{Ra} \ , \qquad (117)
\end{aligned}$$

where $J^a \equiv \int d\vec{x} 2\kappa K F^a_{z0}\Big|_{z=z_c}$ is the unrotated angular momentum in [7]. We note that $R = R_1^T R_2$ and that $R_2^{ab} J^b = -I_2^a$ where I_2^a is the unrotated isovector charge of the nucleon labelled 2. The same holds for label 1. Thus

$$\langle s_1 t_1 s_2 t_2 | V_V | s_1 t_1 s_2 t_2 \rangle \approx \sum_n \frac{1}{4} \psi^2_{2n-1} \frac{e^{-m_{2n-1}d}}{4\pi\, d} \left(\vec{\tau}_1 \cdot \vec{\tau}_2\right) \ , \qquad (118)$$

which is seen to contribute to the isospin part of the central potential

$$V^-_{1,V} \approx \sum_n G^2_{1V,2n-1} \frac{e^{-m_{2n-1}d}}{4\pi\, d} \ , \qquad (119)$$

with $G_{1V,2n-1} = \psi_{2n-1}/2 \approx 1/\sqrt{N_c\lambda}$. This contribution is subleading in the potential.

Similarly, the U(1) vector contribution part (omega, omega', ...) reads

$$V_{\hat{V}} \approx \frac{N_c^2}{16\pi} \sum_n B \psi^2_{2n-1} \frac{e^{-m_{2n-1}d}}{d} B = \frac{N_c^2}{4} \sum_n \psi^2_{2n-1} \frac{e^{-m_{2n-1}d}}{4\pi d} \ , \qquad (120)$$

where $B \equiv \int d\vec{x} \frac{4}{N_c} \kappa K \widehat{F}_{z0}\Big|_{z=z_c}$ is the baryon number introduced in [7]. This contribution to the central potential is leading

$$V_{1,\widehat{V}} \equiv V_{\widehat{V}} \approx \sum_n G^2_{\widehat{V},2n-1} \frac{e^{-m_{2n-1}d}}{4\pi\, d} \ , \tag{121}$$

$$G_{\widehat{V},2n-1} \equiv \frac{N_c}{2} \psi_{2n-1} \ , \tag{122}$$

with $G_{\widehat{V},2n-1} \approx \sqrt{N_c/\lambda}$.

For completeness, we quote the spatial contributions from the vectors, both of which are subleading in the potential. The $SU(2)$ vector meson contribution is

$$V'_V \ = \ 2\kappa^2 K(z_c)^2 \psi_{2n-1}(z_c) \psi_{2m-1}(z_c) \int d\vec{x} d\vec{y} F^a_{iz}(\vec{x}, z_c) \Delta^{mn,ab}_{ij} F^b_{jz}(\vec{y}, z_c) \ . \tag{123}$$

At large separations, the field strength F^a_{iz} splits into two single instantons of relative distance d and flavor orientation $R = R_1^T R_2$. At large relative separation d, (113) simplifies to

$$\begin{aligned} V'_V \ &\approx \ \frac{9}{16\pi} \sum_n J^{ai}_V(0) \left(\psi_{2n-1}\right)^2 \left(-\delta_{ij} + \frac{\partial_i \partial_j}{m^2_{2n-1}}\right) \frac{e^{-m_{2n-1}d}}{d} J^{Raj}_A(0) \\ &= \ \frac{9}{16\pi} \sum_n J^{ai}_V(0) \left(\psi_{2n-1}\right)^2 \left[\left(1 + \frac{2}{m_{2n-1}d} + \frac{3}{m^2_{2n-1}d^2}\right) \widehat{d}_i \widehat{d}_j \right. \\ &\qquad \left. -\delta_{ij} \left(1 + \frac{1}{m^2_{2n-1}d^2}\right)\right] \frac{e^{-m_{2n-1}d}}{d} J^{Raj}_V(0) \ , \end{aligned} \tag{124}$$

where $J^{ai}_V(0) \equiv -(4/3)\kappa K \int d\vec{x} F^a_{iz}$ and the spatial component of the vector current J_V is unrotated while J^R_V is rotated. The projected potential V'_V yields

$$\begin{aligned} &\langle s_1 t_1 s_2 t_2 | V'_V | s_1 t_1 s_2 t_2 \rangle \\ &\quad \approx \frac{g^2_V}{16\pi} \sum_n \left(\psi_{2n-1}\right)^2 e^{-m_{2n-1}d} \left(-\frac{1}{d} - \frac{1}{m^2_{2n-1}d^3}\right) (\vec{\sigma}_1 \cdot \vec{\sigma}_2)\, (\vec{\tau}_1 \cdot \vec{\tau}_2) \\ &\quad\quad + \frac{g^2_V}{16\pi} \sum_n \left(\psi_{2n-1}\right)^2 e^{-m_{2n-1}d} \left(\frac{1}{d} + \frac{2}{m_{2n-1}d^2} + \frac{3}{m^2_{2n-1}d^3}\right) (\vec{\sigma}_1 \cdot \widehat{d})(\vec{\sigma}_2 \cdot \widehat{d})\, (\vec{\tau}_1 \cdot \vec{\tau}_2) \\ &\quad \approx \frac{g^2_V}{16\pi} \sum_n \left(\psi_{2n-1}\right)^2 \frac{e^{-m_{2n-1}d}}{d} \left[(\vec{\sigma}_1 \cdot \widehat{d})(\vec{\sigma}_2 \cdot \widehat{d}) - (\vec{\sigma}_1 \cdot \vec{\sigma}_2)\right] (\vec{\tau}_1 \cdot \vec{\tau}_2) \ , \end{aligned} \tag{125}$$

with $J^{ai}_V(0) = g_V \delta^{ai}$. (125) contributes to both the spin $V'_{S,V}$ and tensor part $V'_{T,V}$ of the NN interaction,

$$\begin{aligned}
V'_{S,V} &\approx \frac{1}{4\pi}\sum_n G^2_{SV,2n-1}\frac{e^{-m_{2n-1}d}}{d} \ , & V'_{T,V} &\approx \frac{1}{4\pi}\sum_n G^2_{TV,2n-1}\frac{e^{-m_{2n-1}d}}{d} \ , \\
G_{SV,2n} &\equiv -\frac{g_V\psi_{2n-1}}{\sqrt{6}} \ , & G_{TV,2n} &\equiv \frac{g_V\psi_{2n-1}}{\sqrt{12}} \ . \qquad (126)
\end{aligned}$$

The holographic description of the nucleon-nucleon potential is consistent with the meson-exchange potentials in nuclear physics. Holography allows a systematic organization of the NN potential in the context of semiclassics, with the NN interaction of order N_c/λ in leading order.

7 Holographic NN potentials

In general, the NN potential in holography is composed of the core and the cloud contributions to order N_c/λ. For non-asymptotic distances, both the core and cloud contributions have a non-linear dependence on the rotation matrix $R(U)$, making the projection on the NN channel involved. Formally, the potential (core plus cloud) can be expanded using the irreducible representations of SU(2). Specifically

$$V(d,U) = \sum_{j=0}^{\infty}\sum_{m=-j}^{+j} V_{jm}(d)\, D^j_{mm}(U) \ , \qquad (127)$$

where $D^j_{m,m'}(U)$ are U-valued Wigner functions. For $k=2$ the azimuthal symmetry restrics $m'=m$ with $V_{jm}=V_{j,-m}$. In particular

$$V_{jm}(d) = \frac{2\pi^2}{(2j+1)}\int dU\, V(d,U)\, D^{j\ *}_{m,m}(U) \ . \qquad (128)$$

The projection on the NN channel follows by sandwiching (127) between the normalized NN states $D^{1/2}(1)\otimes D^{1/2}(2)$. While straightforward, this procedure is involved owing to the complicated nature of the $k=2$ instanton both in the core and in the cloud on $R(U)$. In general

$$V(d,U) = V_{\rm core}(d,U) + V_{\rm cloud}(d,U) \ . \qquad (129)$$

$V_{\rm core}(d,U)$ is defined as

$$\begin{aligned} V_{\rm core}(d,U) &\equiv \Delta E[f_{-+}] - \Delta E[f_-] - \Delta E[f_+] \ , \\ \Delta E[f] &= \frac{\kappa}{6\lambda}\int d^3\widetilde{x} d\widetilde{z} \left(\widetilde{z}^2 - \frac{3^7\pi^2}{2^4} \widetilde{\Box} \log|f| \right) \widetilde{\Box}^2 \log|f| \ , \end{aligned} \tag{130}$$

where

$$\log|f_{-+}| \equiv -\log\left[(g_- + A)(g_+ + A) - B^2 \right] \ , \tag{131}$$

$$\log|f_\pm| = -\log g_\pm \ , \tag{132}$$

$$g_\pm = \sum_{\alpha=2,3,4} \widetilde{x}_\alpha^2 + \left(\widetilde{x}_1 \pm \frac{\widetilde{d}}{2} \right)^2 + \widetilde{\rho}^2 \ , \qquad A = \frac{\widetilde{\rho}^4 \sin^2|\,\theta|}{\widetilde{d}^2} \ , \tag{133}$$

$$B = \widetilde{\rho}^2 \left(\cos|\,\theta| + \frac{2}{\widetilde{d}} \sin|\,\theta| \left[\widehat{\theta}_1 \widetilde{z} + \widehat{\theta}_2 \widetilde{x}_3 - \widehat{\theta}_3 \widetilde{x}_2 \right] \right) \ . \tag{134}$$

$V_{\rm cloud}(d,U)$ is defined as

$$\begin{aligned} V_{\rm cloud}(d,U) &\equiv 2\kappa^2 K^2 \sum_n \psi_n^2 \int d\vec{x} d\vec{y} \\ &\Big[F^a_{iz}(x_M;-+)\Delta_n^{ij}(\vec{x}-\vec{y})\, F^a_{iz}(y_M;-+) + \widehat{F}_{0z}(x_M;-+)\Delta_n^{00}(\vec{x}-\vec{y})\widehat{F}_{0z}(y_M;-+) \\ &\quad -2F^a_{iz}(x_M;-)\Delta_n^{ij}(\vec{x}-\vec{y})\, F^a_{jz}(y_M;-) - 2\widehat{F}_{0z}(x_M;-)\Delta_n^{00}(\vec{x}-\vec{y})\widehat{F}_{0z}(y_M;-) \Big] \Big|_{z=z_c} \ , \end{aligned} \tag{135}$$

where $F^a_{iz}(x_M;-)$ and $F^a_{iz}(x_M;-+)$ are the field strengths of the $k=1$ and the $k=2$ $SU(2)$ instanton respectively,

$$F^a_{iz}(x_M;-) = -2\delta_{ai}\tau^a \frac{\rho^2}{(\xi_-^2+\rho^2)^2} \ , \tag{136}$$

$$\begin{aligned} F^a_{iz}(x_M;-+) &= -2\delta_{ai} U^\dagger \mathbb{B} \left(f_{-+} \otimes \tau^a \right) \mathbb{B}^\dagger U \ , \\ \mathbb{B}^\dagger &= \begin{pmatrix} 0 & -\mathbb{1} & 0 \\ 0 & 0 & -\mathbb{1} \end{pmatrix} \ , \qquad f_{-+}^{-1} = \begin{pmatrix} g_- + A & B \\ B & g_+ + A \end{pmatrix} \ , \\ g_\pm &\equiv x_\alpha^2 + \left(x_1 \pm \frac{d}{2} \right)^2 + \rho^2 \ , \quad x_\alpha^2 \equiv x_2^2 + x_3^2 + x_4^2 \ , \\ A &\equiv \frac{\rho^4 \sin^2|\,\theta|}{d^2} \ , \quad B \equiv \rho^2 \left(\cos|\,\theta| + \frac{2}{d}\sin|\,\theta| \left[\widehat{\theta}_1 z + \widehat{\theta}_2 x_3 - \widehat{\theta}_3 x_2 \right] \right) \ , \\ &\begin{pmatrix} \lambda_1^\dagger & \frac{d}{2}\tau^1 - x^\dagger & \frac{\rho^2}{d}\sin|\,\theta|\,\widehat{\theta}_a \tau^a \tau^1 \\ \lambda_2^\dagger & \frac{\rho^2}{d}\sin|\,\theta|\,\widehat{\theta}_a \tau^a \tau^1 & -\frac{d}{2}\tau^1 - x^\dagger \end{pmatrix} U = 0 \ , \qquad U^\dagger U = \mathbb{1} \ . \end{aligned} \tag{137}$$

The U(1) fields $\widehat{F}_{z0}(x_M;-+)=\partial_z\widehat{A}_0(x_M;-+)$ and $\widehat{F}_{z0}(x_M;-)=\partial_z\widehat{A}_0(x_M;-)$ follow from

$$\widehat{A}_0(x_M;-+)=\frac{1}{32\pi^2 a}\Box\log|f_{-+}|\ ,\qquad \widehat{A}_0(x_M;-)=\frac{1}{32\pi^2 a}\Box\log|f_{-}|\ . \tag{138}$$

The propagators are defined as

$$\Delta_n^{ij}(\vec{x}-\vec{y})=(-\delta_{ij}+\widehat{\partial}_i\widehat{\partial}_j)\frac{e^{-m_n|\vec{x}-\vec{y}|}}{4\pi\,|\vec{x}-\vec{y}|}\ ,\qquad \Delta_n^{00}(\vec{x}-\vec{y})=\frac{e^{-m_n|\vec{x}-\vec{y}|}}{4\pi\,|\vec{x}-\vec{y}|}\ . \tag{139}$$

If we were to saturate (127) by $j=0,1$ which is exact asymptotically as we have shown both for the core and cloud, then the projection procedure is much simpler. In particular, the NN potential simplifies to

$$\begin{aligned}V_{NN}&=V_1^+ +\vec{\tau}_1\cdot\vec{\tau}_2\,V_1^- +\vec{\sigma}_1\cdot\vec{\sigma}_2\left(V_S^+ +\vec{\tau}_1\cdot\vec{\tau}_2\,V_S^-\right) &(140)\\ &+\Big(3(\vec{\sigma}_1\cdot\widehat{d})(\vec{\sigma}_2\cdot\widehat{d})-\vec{\sigma}_1\cdot\vec{\sigma}_2\Big)\left(V_T^+ +\vec{\tau}_1\cdot\vec{\tau}_2\,V_T^-\right)\ , &(141)\end{aligned}$$

with the core contributions

$$\begin{aligned}V^+_{1,\mathrm{core}}&=\frac{1}{4}\left[V(0,0,0)+2V(0,0,\pi/2)+V(\pi/2,0,0)\right]\ , &(142)\\ V^-_{S,\mathrm{core}}&=\frac{1}{4}\left[V(0,0,0)-\frac{2}{3}V(0,0,\pi/2)-\frac{1}{3}V(\pi/2,0,0)\right]\ , &(143)\\ V^-_{T,\mathrm{core}}&=V_T^{11}-V_T^{22}=\frac{1}{6}\left[V(\pi/2,0,0)-V(0,0,\pi/2)\right]\ , &(144)\end{aligned}$$

as detailed above. The cloud contributions V_1, V_S and V_T remain the same. At large distances d the core contribution is dominant and repulsive in the regular gauge (84)

$$V^+_{1,\mathrm{core}}\approx\frac{27\pi N_c}{2\lambda}\frac{1}{d^2}\ , \tag{145}$$

and subdominant and attractive in the singular gauge (161)

$$V^+_{1,\mathrm{core}}\approx-\frac{81\pi N_c}{\lambda^4}\frac{\rho^6}{d^8}\ . \tag{146}$$

The dominant cloud contributions are

$$V^+_{1,\widehat{V}} \approx \sum_n G^2_{1\widehat{V},2n-1} \frac{e^{-m_{2n-1}d}}{4\pi\, d}\ , \qquad G_{1\widehat{V},2n-1} \equiv \frac{N_c}{2}\psi_{2n-1} \ \sim\ \sqrt{\frac{N_c}{\lambda}}\ , \tag{147}$$

$$V^-_{S,A} \approx \sum_n G^2_{SA,2n} \frac{e^{-m_{2n}}d}{4\pi d}\ , \qquad G_{SA,2n} \equiv -\frac{g_A\psi_{2n}}{\sqrt{6}\psi_0} \quad \sim\ \sqrt{\frac{N_c}{\lambda}}\ , \tag{148}$$

$$V^-_{T,A} \approx \sum_n G^2_{TA,2n} \frac{e^{-m_{2n}}d}{4\pi d}\ , \qquad G_{TA,2n} \equiv \frac{g_A\psi_{2n}}{\sqrt{12}\psi_0} \quad \sim\ \sqrt{\frac{N_c}{\lambda}}\ , \tag{149}$$

$$V^-_{T,\Pi} \approx \frac{1}{16\pi}\left(\frac{g_A}{f_\pi}\right)^2 \frac{1}{d^3} \ \sim\ \frac{N_c}{\lambda}\ . \tag{150}$$

from (108), (116), (121), and (119). To order N_c/λ we note that $V_1^- = V_S^+ = V_T^+ = 0$.

8 Conclusions

We have extended the holographic description of the nucleon suggested in [3] to the two nucleon problem. In particular, we have shown how the exact $k = 2$ ADHM instanton configuration applies to the NN problem. The NN potential is divided into a short distance core contribution and a large distance cloud contribution that is meson mediated. This is a first principle description of meson exchange potentials sucessfully used for the nucleon-nucleon problem in pre-QCD [21].

The core contribution in the regular gauge is of order N_c/λ. It is Coulomb like in the central channel. Remarkably, the repulsion is 4-dimensional Coulomb, a hallmark of holography. This repulsion dominates the high baryon density problem in holography as discussed recently in [4, 5]. The dominant Coulomb repulsion is changed to subdominant dipole attraction for instantons in the singular gauge.

We have shown in the context of semiclassics, that the meson-instanton interactions in bulk is strong and of order $\sqrt{N_c/\lambda}$. In the Born-Oppenheimer approximation they contribute to the potentials to order N_c/λ. These cloud contributions dominate at large distances. The central potential is dominated by a tower of omega exchanges, the tensor potential by a tower of pion exchanges, while the spin and tensor potentials are dominated by a tower of axial-vector exchanges. The vector exchanges are subdominant at large N_c and strong coupling. Holography, fixes the potentials at intermediate and short distances without recourse to *adhoc* form factors [21] or truncation as in the Skyrme model [22].

The present work provides a quantitative starting point for an analysis of the NN interaction in strong coupling and large N_c. For a realistic comparison with boson exchange models, we need to introduce a pion mass. It also offers a systematic framework for discussing the deuteron problem, NN form factors and NN-meson and NN-photon emissions in the context of holography. We plan to address some of these issues next.

9 Acknowledgments

We thank Pierre Van Baal, Tamas Kovacs, Larry McLerran and Sang-Jin Sin for discussions. This work was supported in part by US-DOE grants DE-FG02-88ER40388 and DE-FG03-97ER4014.

A Instantons in Singular gauge

The $k = 1$ instanton in the singular gauge follows from (8) through a gauge transformation $g^{-1} = \widehat{\xi} = \xi/|\xi|$ which is singular at $\xi = x - X = 0$. This is achieved through the shift $U \to Ug$, which amounts in general to the new inverse potential $1/f = 1 + \rho^2/\xi_M^2$. The corresponding action density is

$$\mathrm{tr}\, F_{MN}^2 = \Box^2 \log f \; = \frac{96\rho^4}{((x_M - X_M)^2 + \rho^2)^4} - 16\pi^2 \delta(x_M - X_M) \; . \tag{151}$$

The instanton in the singular gauge is threaded by an antiinstanton of zero size at its center. Its topological charge is strictly speaking zero. It is almost 1 if the center $x = X$ is excluded. This point is usually subsumed. Singular instantons have more localized gauge fields than regular instantons.

The ADHM solution for $k = 2$ in singular gauge is not known. Following the $k = 1$ argument, we may seek it from the regular gauge by applying a doubly singular gauge transformation

$$g^{-1} \equiv g_+^{-1}\, g_-^{-1} = \widehat{\xi}_+\, \widehat{\xi}_- \; , \tag{152}$$

which is singular at the centers $\xi_\pm = x \pm D = 0$ in quaternion notations. This amounts to shifting $U \to Ug$ in the ADHM construction. We guess that (152) yields the new inverse potential

$$f^{-1} \to \frac{f^{-1}}{(|x - D||x + D|)} \; , \tag{153}$$

in the singular gauge. As a result, the instanton topological charge is

$$\mathrm{tr}\, F_{MN}^2 = \Box^2 \log f \to \Box^2 \log f - 16\pi^2 \left(\delta(\xi_{+M}) + \delta(\xi_{-M})\right) \ . \tag{154}$$

The $k = 2$ ADHM density is now threaded by two singular anti-instantons at $\xi_\pm = 0$. Singular instantons have more localized gauge fields A_M than regular instantons. While this point is of relevance for gauge variant quantitities, it is irrelevant for gauge invariant quantities with the exception of the topological charge. This point is important for the central nucleon-nucleon potential as we now explain.

B Core in Singular gauge

In the singular gauge we substitute $|f|$ as (153), which results in

$$\Box \log |f| \to \Box \log |f| + \frac{4}{\widetilde{\xi}_+^2} + \frac{4}{\widetilde{\xi}_-^2} \ , \tag{155}$$

$$\Box^2 \log |f| \to \Box^2 \log |f| - 16\pi^2 \Big(\delta(\widetilde{\xi}_{+M}) + \delta(\widetilde{\xi}_{-M})\Big) \ . \tag{156}$$

This gives extra contributions in addition to the result in regular gauge after the subtraction of the self-energy

$$\begin{aligned}
\Delta E &\to \Delta E + \Delta E_s \ , \\
\Delta E_s &\equiv \left(\frac{\kappa}{6\lambda}\right)\left(\frac{3^7\pi^2}{2^4}\right)\int d^3\widetilde{x} d\widetilde{z} \\
&\Big[32\pi^2\big\{\widetilde{\Box}\log|f_\pm|\Big(\delta\widetilde{\xi}_{+M}) + \delta(\widetilde{\xi}_{-M})\Big) - \widetilde{\Box}\log|f_+|\,\delta(\widetilde{\xi}_{+M}) - \widetilde{\Box}\log|f_-|\,\delta(\widetilde{\xi}_{-M})\big\} \\
&+16\pi^2\left(\delta(\widetilde{\xi}_{-M})\frac{4}{\widetilde{\xi}_+^2} + \delta(\widetilde{\xi}_{+M})\frac{4}{\widetilde{\xi}_-^2}\right)\Bigg] \ ,
\end{aligned} \tag{157}$$

which comes from the second term in (70) while the first term in (70) remains the same. $f\pm$, f_+, and f_- are short for the expressions in the regular gauge in (36)-(37). Thus

$$\begin{aligned}
\Delta E_s &= \frac{N_c 27\pi}{8}\left[\int d^3\widetilde{x} d\widetilde{z}\Big[\widetilde{\Box}\log|f|\Big(\delta(\widetilde{\xi}_{+M}) + \delta(\widetilde{\xi}_{-M})\Big)\Big] + \frac{16}{\widetilde{\rho}^2} + \frac{4}{\widetilde{d}^2}\right] \\
&= \frac{N_c 27\pi}{2}\Bigg\{\frac{4}{\widetilde{\rho}^2} + \frac{1}{\widetilde{d}^2} \\
&\quad - 2\widetilde{d}^2\Big[\widetilde{d}^6(2\widetilde{d}^4 + 5\widetilde{d}^2\widetilde{\rho}^2 + 4\widetilde{\rho}^4) + \widetilde{d}^4\widetilde{\rho}^2\cos^2|\theta|\,(-2\widetilde{d}^4 - 4\widetilde{d}^2\widetilde{\rho}^2 - 3\widetilde{\rho}^4\cos(2\,|\theta|))
\end{aligned}$$

$$+2\widetilde{d}^4\widetilde{\rho}^2(\widetilde{d}^4+4\widetilde{d}^2\widetilde{\rho}^2+5\widetilde{\rho}^4)\sin^2|\theta|+\widetilde{d}^2\widetilde{\rho}^6(3\widetilde{d}^2+8\widetilde{\rho}^2)\sin^4|\theta|+2\widetilde{\rho}^{10}\sin^6|\theta|\Big]$$

$$\div\,\widetilde{\rho}^2\Big[\widetilde{d}^4(\widetilde{d}^2+\widetilde{\rho}^2)-\widetilde{d}^4\widetilde{\rho}^2\cos^2|\theta|+\widetilde{d}^2\widetilde{\rho}^2(\widetilde{d}^2+2\widetilde{\rho}^2)\sin^2|\theta|+\widetilde{\rho}^6\sin^4|\theta|\Big]^2\Bigg\} \tag{158}$$

$$= \; -\left(\frac{N_c 27\pi}{2\lambda}\right)\frac{1+4\cos(2\,|\theta|)}{d^2}+\mathcal{O}(d^{-4}) \qquad (d\gg 1)\ . \tag{159}$$

For large d, the monopole contribution in (158) is cancelled by the monopole contribution (84) in the regular gauge. This cancellation leads to a dipole attraction in the singular gauge.

The net dipole attraction in the singular gauge is best seen by noting that (83) now reads

$$V_D \approx -2bcN_c\int\left(\widetilde{\Box}^2\log\left(1+\widetilde{\rho}^2/\widetilde{\xi}_+^2\right)\right)\frac{1}{\widetilde{\Box}}\left(\widetilde{\Box}^2\log\left(1+\widetilde{\rho}^2/\widetilde{\xi}_-^2\right)\right)\ , \tag{160}$$

where $\widetilde{x}_\pm$ refers to the shifted instanton positions. For large separations $\widetilde{d}/\widetilde{\rho}\gg 1$, the leading contribution to V_D is

$$V_D \approx -768\pi^2\,bc\,N_c\,\frac{\widetilde{\rho}^6}{\widetilde{d}^8} = -81\pi N_c\frac{\widetilde{\rho}^6}{\widetilde{d}^8}\ , \tag{161}$$

by repeated use of the 4-dimensional formulae

$$\Box\,\frac{1}{\xi^{2n}} = -4\pi^2\,\delta_{n1}\,\delta^4(\xi)+2n(2(n+1)-4)\frac{1}{\xi^{2(n+1)}}\ . \tag{162}$$

This contribution is of order N_c/λ^4 following the unscaling of $\widetilde{d}=\sqrt{\lambda}d$. (161) is dipole-like and attractive. As expected, the threading antiinstanton in the singular gauge cancels the leading N_c/λ repulsive monopole contribution in 4-dimensional Coulomb's law, resulting in the attractive dipole-like contribution (van der Waals).

C Strong Source Theory

In this Appendix, we check our cloud calculation in the singular gauge using the strong coupling source theory used for small cores in [20, 23] and more recently in holography in [6]. This method provides an independent check on our semiclassics in the $k=2$ sector.

The energy in the leading order of λ is

$$E=\kappa\ \mathrm{tr}\int d^3x dz\left(\frac{1}{2}K^{-1/3}F_{ij}^2+KF_{iz}^2\right)+\frac{\kappa}{2}\int d^3x dz\left(\frac{1}{2}K^{-1/3}\widehat{F}_{ij}^2+K\widehat{F}_{iz}^2\right)\ . \tag{163}$$

where, in the region $1 \ll \xi$,

$$\widehat{A}_0 \approx -\frac{1}{2a\lambda}(G_- + G_+) \ , \tag{164}$$

$$A_i^a \approx -2\pi^2\rho^2 \left(\left(\epsilon^{iaj}\partial_{+j} - \delta^{ia}\partial_{+Z}\right) G_+ + R^{ab}\left(\epsilon^{ibj}\partial_{-j} - \delta^{ib}\partial_{-Z}\right) G_- \right) \ , \tag{165}$$

$$A_z^a \approx -2\pi^2\rho^2 \left(\partial_{+a}H_+ + R^{ab}\partial_{-b}H_-\right) \ , \tag{166}$$

with

$$G_\pm \approx \kappa \sum_{n=1}^{\infty} \psi_n(z)\psi_n(\pm Z) Y_n\left(\left|\vec{x} - \vec{X}_\pm\right|\right) \ , \tag{167}$$

$$H_\pm \approx \kappa \sum_{n=0}^{\infty} \phi_n(z)\phi_n(\pm Z) Y_n\left(\left|\vec{x} - \vec{X}_\pm\right|\right) \ , \tag{168}$$

$$\phi_0(z) \equiv \frac{1}{\sqrt{\kappa\pi}K(z)} \ , \quad \phi_n(z) = \frac{1}{\sqrt{\lambda_n}}\partial_z\psi_n(z) \quad (n = 1, 2, 3, \cdots) \ , \tag{169}$$

$$Y_n\left(\left|\vec{x} - \vec{X}_\pm\right|\right) \equiv -\frac{e^{-\sqrt{\lambda_n}\left|\vec{x}-\vec{X}_\pm\right|}}{4\pi\left|\vec{x} - \vec{X}_\pm\right|} \ , \quad \partial_{\pm a} \equiv \frac{\partial}{\partial X_\pm^a} \ , \quad \partial_{\pm Z} \equiv \frac{\partial}{\partial Z_\pm} \ . \tag{170}$$

C.1 Pion

The pion contribution stems from

$$E_\Pi = \frac{\kappa}{2}\int d^3x dz K \left(\partial_i A_z^a\right)\left(\partial_i A_z^a\right) \ , \tag{171}$$

where

$$A_z^a \approx -2\pi^2\rho^2 \left(\partial_{+a}H_+ + R^{ab}\partial_{-b}H_-\right) \ , \tag{172}$$

with $\phi_0(z)$ only. After subtracting the self-energy the pion interaction energy (V_Π) is

$$\begin{aligned} V_\Pi &= \kappa\left(2\pi^2\rho^2\right)^2 R^{ab}\int d^3x dz K \left(\partial_i\partial_{+a}H_+\right)\left(\partial_i\partial_{-b}H_-\right) \\ &\approx \frac{1}{2\,3^2\pi}\frac{N_c\lambda\rho^4}{d^3}R^{ab}\left(\widehat{d}_a\widehat{d}_b - \frac{\delta_{ab}}{3}\right) \ , \end{aligned} \tag{173}$$

after using $2\partial_a = -\partial_{\pm a}$ and dropping the surface terms. $\vec{X}_+ = -\vec{X}_- = \frac{\vec{d}}{2}$ and $Z_c \approx 0$. The matrix element of (173) in the 2-nucleon state is

$$
\begin{aligned}
\langle s_1 s_2 t_1 t_2 | V_{\Pi} | s_1 s_2 t_1 t_2 \rangle &= \frac{1}{2\,3^5 \pi} \frac{N_c \lambda \rho^4}{d^3} \left(3(\vec{\sigma}_1 \cdot \widehat{d})(\vec{\sigma}_2 \cdot \widehat{d}) - \vec{\sigma}_1 \cdot \vec{\sigma}_2 \right) (\vec{\tau}_1 \cdot \vec{\tau}_2) \\
&\equiv \frac{1}{4M^2} \frac{g_{\pi NN}^2}{4\pi} \frac{1}{d^3} \left(3(\vec{\sigma}_1 \cdot \widehat{d})(\vec{\sigma}_2 \cdot \widehat{d}) - \vec{\sigma}_1 \cdot \vec{\sigma}_2 \right) (\vec{\tau}_1 \cdot \vec{\tau}_2) \ , \qquad (174)
\end{aligned}
$$

after using $\langle s_1 s_2 t_1 t_2 | R^{ab} | s_1 s_2 t_1 t_2 \rangle = \frac{1}{9} \sigma_1^a \sigma_2^b \vec{\tau}_1 \cdot \vec{\tau}_2$. The last equality follows from the canonical $\pi\, N$ pseudovector coupling. Thus

$$
\left(\frac{g_{\pi NN}}{M} \right)^2 = \frac{8 N_c \lambda \rho^4}{3^5} = \left(\frac{\widehat{g}_A}{f_\pi} \right)^2 \ , \qquad (175)
$$

where $\widehat{g}_A = \frac{64}{3} \kappa \pi \rho^2$ obtained in [6], and $f_\pi^2 = 4\kappa/\pi$. This is just the Goldberger-Treiman relation following from the NN interaction using the strongly coupled source approximation [6]. As noted in Appendix D, our normalization of the axial-vector current appears to be twice the normalization of the same current used in [6].

C.2 Omega

The ω contribution stems from

$$
E_{\widehat{V}} = \frac{\kappa}{2} \int d^3x dz K \left(\partial_z \widehat{A}_0 \right) \left(\partial_z \widehat{A}_0 \right) \ , \qquad (176)
$$

where

$$
\widehat{A}_0 \approx - \frac{1}{2a\lambda} (G_- + G_+) \ . \qquad (177)
$$

After subtracting the self-energy the ω interaction energy ($V_{\widehat{V}}$) is

$$
\begin{aligned}
V_{\widehat{V}} &= \frac{\kappa^2 \psi_n(Z_+) \psi_n(Z_-) m_{2n-1}^2}{(2a\lambda 4\pi)^2} \int d\vec{x} \; \frac{e^{-m_{2n-1}\left(|\vec{x} - \vec{X}_-| + |\vec{x} - \vec{X}_+| \right)}}{|\vec{x} - \vec{X}_-| |\vec{x} - \vec{X}_+|} \qquad (178) \\
&\approx \frac{N_c^2}{(8\pi)^2} \psi_n^2 m_{2n-1}^2 \int dr (4\pi r^2) \; \frac{e^{-m_{2n-1}(r+d)}}{rd} \qquad (179) \\
&\approx \frac{N_c}{4} \sum_n \psi_{2n-1}^2 \frac{e^{-m_{2n-1} d}}{4\pi d} \ , \qquad (180)
\end{aligned}
$$

where we used

$$\kappa \int dz K(z) \partial_z \psi_n(z) \partial_z \psi_m(z) = m_{2n-1}^2 \delta_{nm} \ . \tag{181}$$

The result is in agreement with (120). At large separations, the strongly coupled source theory and the semiclassical quantization yields the same results. This outcome is irrespective of the use of the singular gauge (strong coupling) or regular gauge (semiclassics). This a consequence of gauge invariance.

At short distances, gauge invariance is upset by the delta-function singularities present in the singular gauge. Indeed, for $\rho \ll \xi \ll 1$ the omega contribution stems from

$$E_{\widehat{V}} = \frac{\kappa}{2} \int d^3x dz K \left(\partial_z \widehat{A}_0 \right) \left(\partial_z \widehat{A}_0 \right) \ , \tag{182}$$

with now $K \approx 1$ and

$$\begin{aligned} \widehat{A}_0 &\approx -\frac{1}{2a\lambda} (G_-^{\text{flat}} + G_+^{\text{flat}}) \ , && (183) \\ G_\pm^{\text{flat}} &= -\frac{1}{4\pi^2} \frac{1}{\xi_\pm^2} \ , && (184) \end{aligned}$$

from [6]. After subtracting the self-energy the ω interaction energy ($V'_{\widehat{V}}$) is

$$\begin{aligned} V'_{\widehat{V}} &= \frac{\kappa}{(2a\lambda 4\pi)^2} \int d\vec{x} dz \frac{4z^2}{\left((x_1 - d/2)^2 + x_\alpha^2 \right)^2 \left((x_1 + d/2)^2 + x_\alpha^2 \right)^2} \\ &= \frac{27 N_c}{2\pi \lambda d^2} \int d\vec{x} dz \frac{z^2}{\left((x_1 - 1/2)^2 + x_\alpha^2 \right)^2 \left((x_1 + 1/2)^2 + x_\alpha^2 \right)^2} \\ &\approx \frac{27\pi N_c}{4\lambda d^2} \ . \end{aligned} \tag{185}$$

We have rescaled the variable $x_M \to x_M/d$ in the second line and carried numerically the integration through

$$\int d\vec{x} dz \frac{z^2}{\left((x_1 - 1/2)^2 + x_\alpha^2 \right)^2 \left((x_1 + 1/2)^2 + x_\alpha^2 \right)^2} \approx 4.9348 \approx \frac{\pi^2}{2} \ . \tag{186}$$

The omega repulsion at short distance is about $V_{\widehat{V}}/2$ in (84). The discrepancy may be due to the singularities introduced in the singular gauge and/or the approximation in the matching region $\rho \ll \xi \ll 1$. It is worth noting that the standard omega repulsion at large ditances (180) transmutes to a 4-dimensional Coulomb repulsion in holography.

D Axial Form Factor

The effective action for the SU(2)-valued axial vectors to order $\hbar^0$ follows from [7]

$$S_{\rm eff}[\mathscr{A}^a_\mu] = \sum_{b=1}^{3}\sum_{n=1}^{\infty}\int d^4x \left[-\frac{1}{4}\Big(\partial_\mu a^{b,n}_\nu - \partial_\nu a^{b,n}_\mu\Big)^2 - \frac{1}{2}m^2_{a^n}(a^{b,n}_\mu)^2\right.$$

$$-\kappa K \mathbb{F}^{b,z\mu}\mathscr{A}^b_\mu(\psi_0 - \alpha_{a^n}\psi_{2n})\Big|_{z=B}$$

$$\left. + \, a_{a^n}m^2_{a^n}a^{b,n}_\mu\mathscr{A}^{b,\mu} - \kappa K\mathbb{F}^{b,z\mu}a^{b,n}_\mu\psi_{2n}\Big|_{z=B}\right] \, , \tag{187}$$

The first line is the free action of the massive axial vector meson which gives the meson propagator

$$\Delta^{mn,ab}_{\mu\nu}(x) = \int\frac{d^4p}{(2\pi)^4}e^{-ipx}\left[\frac{-g_{\mu\nu} - p_\mu p_\nu/m^2_{a^n}}{p^2 + m^2_{a^n}}\delta^{mn}\delta^{ab}\right] \, , \tag{188}$$

in Lorentz gauge. The rest are the coupling terms between the source and the instanton: the second line is the direct coupling and the last line corresponds to the coupling mediated by the $SU(2)$ (a, a', ...) vector meson couplings,

$$\kappa K\mathbb{F}^{b,z\mu}a^{b,n}_\mu\psi_{2n} \, , \tag{189}$$

which is large and of order $1/\sqrt{\hbar}$ since $\psi_{2n} \sim \sqrt{\hbar}$. When ρ is set to $1/\sqrt{\lambda}$ after the bookkeeping noted above, the coupling scales like $\lambda\sqrt{N_c}$, or $\sqrt{N_c}$ in the large N_c limit taken first

The direct coupling drops by the sum rule

$$\sum_{n=1}^{\infty}\alpha_{a^n}\psi_{2n} = \psi_0 \; = \frac{2}{\pi}\arctan z, \tag{190}$$

following from closure in curved space

$$\delta(z - z') = \sum_{n=1}^{\infty} \; \kappa\psi_n(z)\psi_n(z')K^{-1/3}(z') \, . \tag{191}$$

in complete analogy with VMD for the pion [11] and the electromagnetic baryon form factor [7]. It follows form (190) that

$$\sum_{n=1}^{\infty} \alpha_{a^n} \psi_{2n}(z_c) = \frac{1}{2} \int_{-z_c}^{z_c} dz \partial_z \psi_0(z) = \frac{\kappa}{\pi} \int_{-z_c}^{z_c} dz \phi_0(z) \ . \tag{192}$$

The axial vector contributions at the core sum up to the axial zero mode.

The iso-axial current is,

$$J^{\mu}_{A,b}(x) = -\sum_{n,m} m^2_{a^n} a_{a^n} \psi_{2n} \int d^4y \ \ \mathbb{Q}^b_{\nu}(y,z) \Delta^{\nu\mu}_{mn}(y-x) \Big|_{z=B} \ , \tag{193}$$

with

$$\mathbb{Q}^b_{\nu}(y,z) \equiv \kappa K \mathbb{F}^b{}_{z\nu}(y,z) \ . \tag{194}$$

The static axial-iso-vector form factor follows readily in the form

$$\begin{aligned} J^{bi}_A(\vec{q}) &= \int d\vec{x} e^{i\vec{q}\cdot\vec{x}} J^{bi}_A(x) \\ &= (\delta^{ij} - \hat{q}^i \hat{q}^j) \int d\vec{x} e^{i\vec{q}\cdot\vec{x}} \sum_n \frac{\alpha_{a^n} m^2_{a^n}}{\vec{q}^{\ 2} + m^2_{a^n}} \psi_{2n}(z)\, \mathbb{Q}^b_j(\vec{x},z) \Big|_{z=B} \ , \end{aligned} \tag{195}$$

and is explicitly transverse for massless pions. The zero momentum limit of the transverse momentum projector is ambiguous owing to the divergence of the spatial integrand for $\vec{q} = \vec{0}$. We use the rotationally symmetric limit with the convention $(\delta^{ij} - \hat{q}^i \hat{q}^j) \to 2\delta^{ij}/3$. Thus

$$J^{bi}_A(0) = \frac{2}{3} \int d\vec{x}\, \kappa K \mathbb{F}^b{}_{zi}(\vec{x},z) \psi_0(z) \Big|_{z=B} \ , \tag{196}$$

by the sum rule (192). Since the rotated instanton yields

$$\int d\vec{x}\, \mathbb{F}^{R,a}_{zi} = R^{ai} \frac{4\pi^2 \rho^2}{\sqrt{z_c^2 + \rho^2}} \ , \tag{197}$$

the spatial component of the axial-vector reads

$$J^{Rbi}_A(0) = \frac{32\kappa\pi\rho^2}{3} (1 + z_c^2) \frac{\arctan(z_c)}{\sqrt{\rho^2 + z_c^2}}\, R^{bi} \ , \tag{198}$$

In the nucleon state

$$\begin{aligned}\langle s't'|J_A^{Rbi}(0)|st\rangle &= \frac{32\kappa\pi\rho^2(1+z_c^2)}{9\sqrt{\rho^2+z_c^2}}\arctan(z_c)(\sigma^b)^{ss'}(\tau^i)^{tt'} \\ &\equiv \frac{1}{3}g_A(\sigma^b)^{ss'}(\tau^i)^{tt'}\ , \end{aligned} \tag{199}$$

where we used $\langle s't'|R^{bi}|st\rangle = -\frac{1}{3}(\sigma^b)^{ss'}(\tau^i)^{tt'}$. Thus

$$g_A = \frac{32\kappa\pi\rho^2(1+z_c^2)}{3\sqrt{\rho^2+z_c^2}}\arctan(z_c) \approx \frac{32}{3}\kappa\pi\rho^2\ , \tag{200}$$

where the limit $\rho \to 0$ is followed by $z_c \to 0$. It is 2 times $\widehat{g}_A = \frac{16}{3}\kappa\pi\rho^2$ as quoted in [6]. This discrepancy maybe traced back to a factor of 2 discrepancy in the normalization of the axial-vector current in [6].

References

[1] S. J. Brodsky and G. F. de Teramond, "Light-Front Dynamics and AdS/QCD: The Pion Form Factor in the Space- and Time-Like Regions," arXiv:0707.3859 [hep-ph]; S. J. Brodsky and G. F. de Teramond, "AdS/CFT and Exclusive Processes in QCD," arXiv:0709.2072 [hep-ph].

[2] D. K. Hong, M. Rho, H. U. Yee and P. Yi, "Chiral dynamics of baryons from string theory," arXiv:hep-th/0701276; D. K. Hong, M. Rho, H. U. Yee and P. Yi, "Dynamics of Baryons from String Theory and Vector Dominance," arXiv:0705.2632 [hep-th]; D. K. Hong, M. Rho, H. U. Yee and P. Yi, "Nucleon Form Factors and Hidden Symmetry in Holographic QCD," arXiv:0710.4615 [hep-ph]; J. Park and P. Yi, "A Holographic QCD and Excited Baryons from String Theory," arXiv:0804.2926 [hep-th]; M. Rho, "Baryons and Vector Dominance in Holographic Dual QCD," arXiv:0805.3342 [hep-ph]; D. Gazit and H. U. Yee, "Weak-Interacting Holographic QCD," Phys. Lett. B **670**, 154 (2008) [arXiv:0807.0607 [hep-th]].

[3] H. Hata, T. Sakai, S. Sugimoto and S. Yamato, "Baryons from instantons in holographic QCD," arXiv:hep-th/0701280.

[4] K. Y. Kim, S. J. Sin and I. Zahed, "Dense hadronic matter in holographic QCD," arXiv:hep-th/0608046; K. Y. Kim, S. J. Sin and I. Zahed, "The Chiral Model of Sakai-

Sugimoto at Finite Baryon Density," arXiv:0708.1469 [hep-th]; K. Y. Kim, S. J. Sin and I. Zahed, "Dense and Hot Holographic QCD: Finite Baryonic E Field," arXiv:0803.0318 [hep-th]; K. Y. Kim and I. Zahed, "Baryonic Response of Dense Holographic QCD," arXiv:0811.0184 [hep-th].

[5] K. Y. Kim, S. J. Sin and I. Zahed, "Dense Holographic QCD in the Wigner-Seitz Approximation," arXiv:0712.1582 [hep-th].

[6] K. Hashimoto, T. Sakai and S. Sugimoto, "Holographic Baryons : Static Properties and Form Factors from Gauge/String Duality," arXiv:0806.3122 [hep-th].

[7] K. Y. Kim and I. Zahed, "Electromagnetic Baryon Form Factors from Holographic QCD," JHEP **0809**, 007 (2008) [arXiv:0807.0033 [hep-th]].

[8] H. Hata, M. Murata and S. Yamato, "Chiral currents and static properties of nucleons in holographic QCD," arXiv:0803.0180 [hep-th]; K. Hashimoto, "Holographic Nuclei," arXiv:0809.3141 [hep-th]; S. Seki and J. Sonnenschein, "Comments on Baryons in Holographic QCD," arXiv:0810.1633 [hep-th].

[9] K. Nawa, H. Suganuma and T. Kojo, "Baryons in Holographic QCD," Phys. Rev. D **75**, 086003 (2007) [arXiv:hep-th/0612187]; K. Nawa, H. Suganuma and T. Kojo, "Brane-induced Skyrmions: Baryons in holographic QCD," Prog. Theor. Phys. Suppl. **168**, 231 (2007) [arXiv:hep-th/0701007]; K. Nawa, H. Suganuma and T. Kojo, "Baryons with holography," arXiv:0806.3040 [hep-th]; K. Nawa, H. Suganuma and T. Kojo, "Baryonic matter in holographic QCD," arXiv:0806.3041 [hep-th]; H. Suganuma, K. Nawa and T. Kojo, "Baryons and Baryonic Matter in Holographic QCD from Superstring," arXiv:0809.0805 [hep-th]; K. Nawa, H. Suganuma and T. Kojo, "Brane-induced Skyrmion on S^3: baryonic matter in holographic QCD," arXiv:0810.1005 [hep-th];

[10] N. Horigome and Y. Tanii, "Holographic chiral phase transition with chemical potential," JHEP **0701**, 072 (2007) [arXiv:hep-th/0608198]; O. Bergman, G. Lifschytz and M. Lippert, "Holographic Nuclear Physics," arXiv:0708.0326 [hep-th]; M. Rozali, H. H. Shieh, M. Van Raamsdonk and J. Wu, "Cold Nuclear Matter In Holographic QCD," arXiv:0708.1322 [hep-th].

[11] T. Sakai and S. Sugimoto, "Low energy hadron physics in holographic QCD," Prog. Theor. Phys. **113**, 843 (2005) [arXiv:hep-th/0412141]; T. Sakai and S. Sugimoto, "More

on a holographic dual of QCD," Prog. Theor. Phys. **114**, 1083 (2006) [arXiv:hep-th/0507073].

[12] A. Jackson, A. D. Jackson and V. Pasquier, "The Skyrmion-Skyrmion Interaction," Nucl. Phys. A **432** (1985) 567; R. Vinh Mau, M. Lacombe, B. Loiseau, W. N. Cottingham and P. Lisboa, "The Static Baryon Baryon Potential In The Skyrme Model," Phys. Lett. B **150**, 259 (1985).

[13] M. Oka, "The nuclear force in the Skyrme model," Phys. Rev. C **36**, 720 (1987).

[14] H. Yamagishi and I. Zahed, "Nucleon-nucleon Hamiltonian from Skyrmions," Phys. Rev. D **43**, 891 (1991); V. Thorsson and I. Zahed, "Central Nucleon-Nucleon Potential From Skyrmions," Phys. Rev. D **45**, 965 (1992).

[15] M. Garcia Perez, T. G. Kovacs and P. van Baal, "Comments on the instanton size distribution," Phys. Lett. B **472**, 295 (2000) [arXiv:hep-ph/9911485]; M. Garcia Perez, T. G. Kovacs and P. van Baal, "Overlapping instantons," arXiv:hep-ph/0006155.

[16] M. F. Atiyah, N. J. Hitchin, V. G. Drinfeld and Yu. I. Manin, "Construction of instantons," Phys. Lett. A **65** (1978) 185.

[17] N. H. Christ, E. J. Weinberg and N. K. Stanton, "General self-dual Yang-Mills solutions," Phys. Rev. D **18**, 2013 (1978); A. Actor, "Classical Solutions Of SU(2) Yang-Mills Theories," Rev. Mod. Phys. **51**, 461 (1979); N. Dorey, V. V. Khoze and M. P. Mattis, "Multi-Instanton Calculus in N=2 Supersymmetric Gauge Theory," Phys. Rev. D **54**, 2921 (1996) [arXiv:hep-th/9603136]; N. Dorey, T. J. Hollowood, V. V. Khoze and M. P. Mattis, "The calculus of many instantons," Phys. Rept. **371**, 231 (2002) [arXiv:hep-th/0206063].

[18] H. Osborn, "Calculation Of Multi - Instanton Determinants," Nucl. Phys. B **159**, 497 (1979).

[19] E. Braaten and L. Carson, "The deuteron as a toroidal Skyrmion", Phys. Rev. **D38**, 3525 (1988)

[20] G. F. Chew, "Renormalization of Meson Theory with a Fixed Extended Source," Phys. Rev. **94**, 1748 (1954).

[21] G. E. Brown and A. D. Jackson, "The Nucleon-Nucleon Interaction," North-Holland, Amsterdam, 1976. (References therein)

[22] I. Zahed and G. E. Brown, “The Skyrme Model,” Phys. Rept. **142**, 1 (1986).

[23] J. A. Parmentola, “Static Bag Source Meson Field Theory: Strong Coupling Approximation,” Phys. Rev. D **27**, 2686 (1983); J. A. Parmentola, “Some Implications Of A Small Bag Radius,” Phys. Rev. D **29**, 2563 (1984).